

Annual Thesis Committee (TC) meeting

July 10, 2022

Arpit Babbar

Main developments

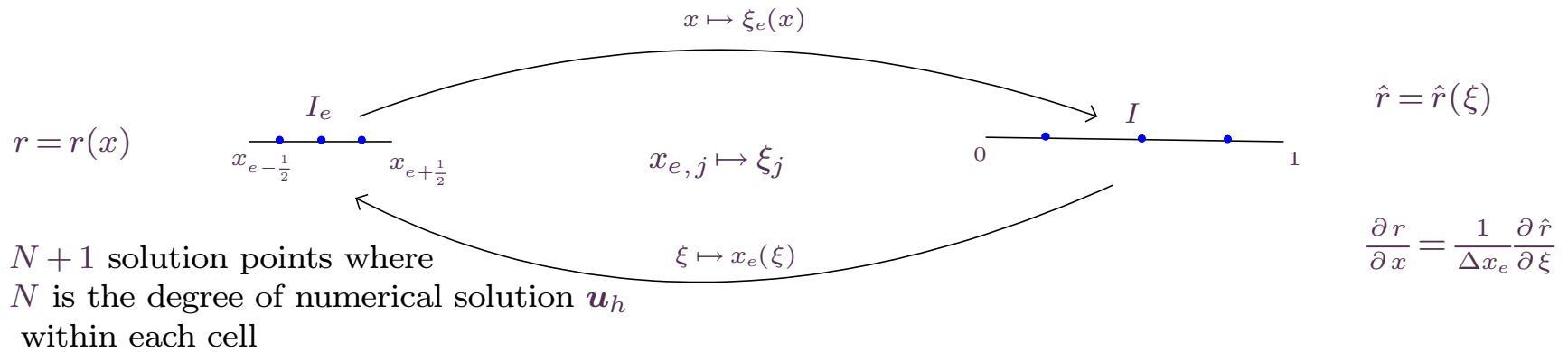
- Extended Zhang-Shu's positivity limiter [20] to Lax-Wendroff schemes to obtain a provably admissibility preserving Lax-Wendroff scheme
- Developed blending limiter of Hennemann Et Al [5] for Lax-Wendroff schemes. Improved the lower order part of blending from first order finite volume method to second order MUSCL-Hancock method.
- Extended proof of admissibility of MUSCL-Hancock method by Berthon [1] to non-cell centred finite volume grids used by [5]. Used a problem independent procedure to limit slope for admissibility.
- Made theoretical comparison of Lax-Wendroff and ADER schemes - proved equivalence for linear case with D2 dissipation and *closeness* for non-linear case.

Structure of presentation

- Review of Lax-Wendroff Flux Reconstruction with D2 dissipation numerical flux.
- Brief introduction to the blending limiter of [5].
- Extending Zhang-Shu's limiter [20] to Lax-Wendroff schemes.
- Admissibility preserving MUSCL-Hancock reconstruction on non-cell centred grids used by [5].
- Prove equivalence of ADER and LW-D2 schemes with numerical verification, also recall instability issues noted in RKDG schemes by Xu Et Al in [19].
- Numerical results demonstrating admissibility preservation and accuracy improvement of limiting procedure.
- Summary and future plans

Flux Reconstruction (FR) by Huynh [6]

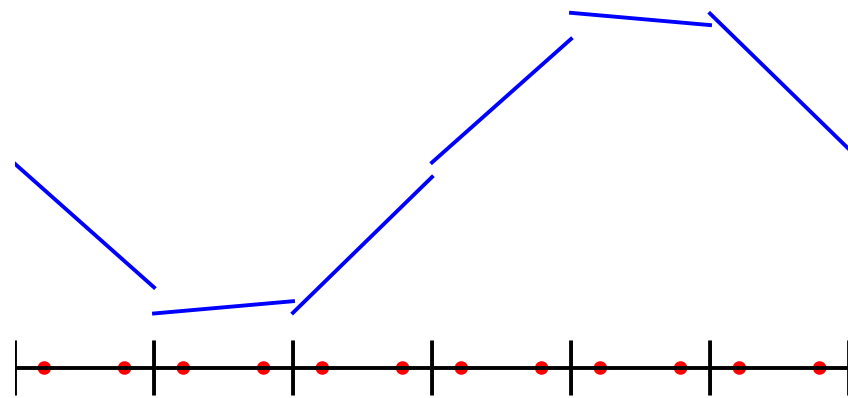
$$\mathbf{u}_t + \mathbf{f}(\mathbf{u})_x = 0$$



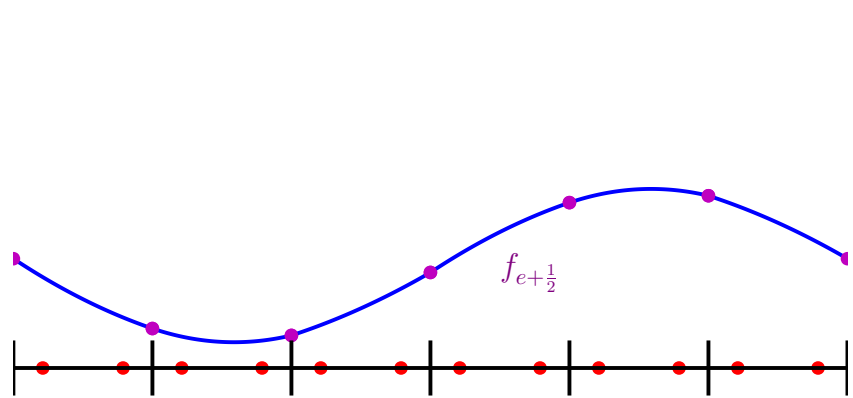
Flux Reconstruction (FR) by Huynh [6]

$$\frac{d}{dt} u_{e,i} = -\frac{\partial f_h}{\partial x}(x_{e,i}), \quad 1 \leq i \leq N+1.$$

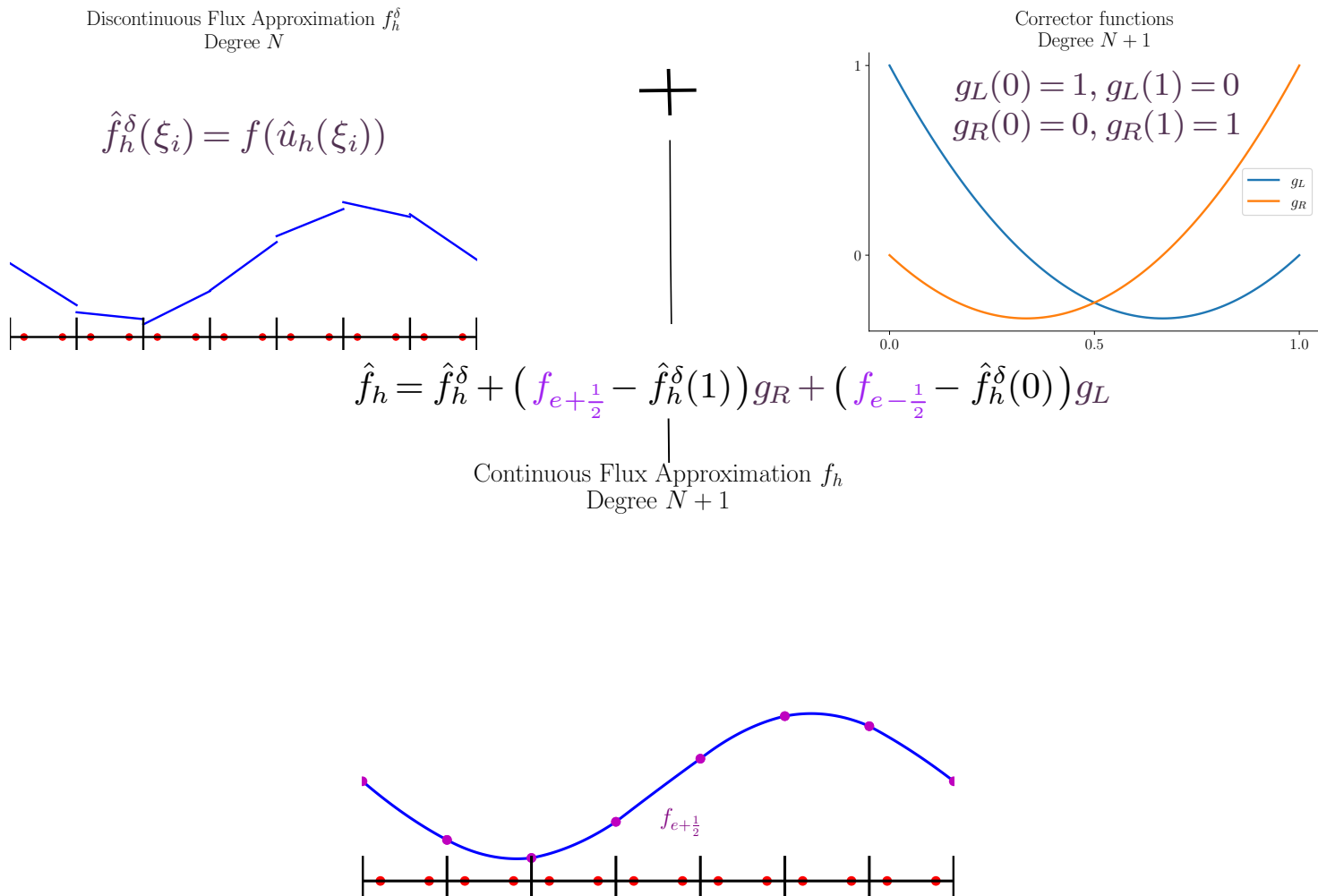
Degree N approximate solution u_h



Degree $N+1$ Continuous Flux Approximation f_h



Flux Reconstruction (FR) by Huynh [6]



Lax-Wendroff Flux Reconstruction (LWFR) with D2 dissipation

$$u^{n+1} = u^n - \Delta t F_x^n,$$

where $F = f(u) + \frac{\Delta t}{2}(f(u))_t + \frac{\Delta t^2}{3!}f(u)_{tt} + \dots + \frac{\Delta t^N}{(N+1)!}\frac{\partial^N}{\partial t^N}f(u)$

To compute F , we use the approximate Lax-Wendroff procedure proposed by Zorio Et Al. [21]

$$\begin{aligned} f(u)_t &\approx \frac{f(u(x, t + \Delta t)) - f(u(x, t - \Delta t))}{2\Delta t} + O(\Delta t^2) \\ &\approx \frac{f(u + \Delta t \mathbf{u}_t) - f(u - \Delta t \mathbf{u}_t)}{2\Delta t} + O(\Delta t^2), \end{aligned}$$

and $\mathbf{u}_t = -f(u)_x$.

This will give us a discontinuous flux polynomial F_h^δ which we will correct with Flux Reconstruction (FR) using numerical flux $F_{e+\frac{1}{2}}$ and denote corrected flux by F_h .

In the past works, $F_{e+\frac{1}{2}}$ has been computed as

$$\begin{aligned} F_{e+\frac{1}{2}} &= F(F_L, F_R, u_L, u_R), \\ u_L &= u_h(x_{e+1/2}^-), \quad u_R = u_h(x_{e+1/2}^+). \end{aligned}$$

In cite, we propose the **Dissipation 2** flux

$$u_L = U_h(x_{e+1/2}^-), \quad u_R = U_h(x_{e+1/2}^+),$$

where

$$U_h = u + \frac{\Delta t}{2}u_t + \frac{\Delta t^2}{3!}u_{tt} + \dots + \frac{\Delta t^N}{(N+1)!}\frac{\partial^N}{\partial t^N}u \approx \frac{1}{\Delta t} \int_{t^n}^{t^{n+1}} u_h dt.$$

Conservation property of LWFR

$$(u_j^e)^{n+1} = (u_j^e)^n - \frac{\Delta t}{\Delta x_e} \frac{\partial F_h}{\partial \xi}(\xi_j), \quad 1 \leq j \leq N+1.$$

For $\{w_j\}_{j=1}^{N+1}$ being the quadrature weights associated to solution points,

$$\begin{aligned} \sum_{j=1}^{N+1} w_j (u_j^e)^{n+1} &= \sum_{j=1}^{N+1} (u_j^e)^n - \frac{\Delta t}{\Delta x_e} \sum_{j=1}^{N+1} w_j \frac{\partial F_h}{\partial \xi}(\xi_j), \\ \Rightarrow \bar{u}_e^{n+1} &= \bar{u}_e^n - \frac{\Delta t}{\Delta x_e} \left[F_{e+\frac{1}{2}} - F_{e-\frac{1}{2}} \right] \end{aligned}$$

We call this the **conservation property**.

Blending limiter

Here we apply the Blending limiter of Hennemann Et Al. [5] to the LWFR scheme. The update for a **high order** LWFR method can be written as

$$\mathbf{u}_e^{H,n+1} = \mathbf{u}_e^n - \frac{\Delta t}{\Delta x_e} \mathbf{R}_e^H.$$

The update for a **lower order** subcell method (like FO FVM or MUSCL-Hancock method) is given by

$$\mathbf{u}_e^{L,n+1} = \mathbf{u}_e^n - \frac{\Delta t}{\Delta x_e} \mathbf{R}_e^L.$$

Then, defining the **blended** residual

$$\mathbf{R}_e = (1 - \alpha_e) \mathbf{R}_e^H + \alpha_e \mathbf{R}_e^L,$$

the **limited** update is performed as

$$\mathbf{u}_e^{n+1} = \mathbf{u}_e^n - \frac{\Delta t}{\Delta x_e} \mathbf{R}_e.$$

Choice of α_e : Smoothness indicator

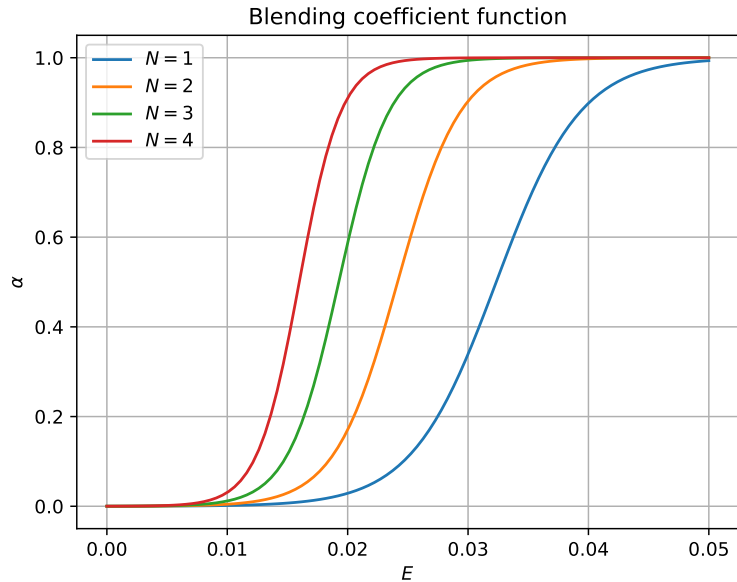
We compute α_e as proposed by Gassner Et Al. [5]. For a degree N polynomial $\epsilon = \epsilon(\xi)$, we can perform an expansion in the orthonormal Legendre basis

$$\epsilon = \sum_{j=1}^{N+1} m_j L_j, \quad m_j = \langle \epsilon, L_j \rangle_{L^2},$$

and define the energy content of ϵ to be

$$\mathbb{E} = \max \left(\frac{m_{N+1}^2}{\beta_1 m_1 + \sum_{j=2}^{N+1} m_j^2}, \frac{m_N^2}{\beta_2 m_1 + \sum_{j=2}^N m_j^2} \right).$$

Smoothness indicators of this kind were first introduced by Persson and Peraire [11]. In the literature, the choice of $\beta_1 = \beta_2 = 1$ has been made. Our experiments reveal that the optimal choice of β_i 's is problem dependent.



$$\epsilon = \rho p$$

$$\alpha(\mathbb{E}) = \frac{1}{1 + \exp(-\frac{s}{T}(\mathbb{E} - T))}$$

where

$$T(N) = 0.5 \cdot 10^{-1.8(N+1)^{1/4}}, \quad \alpha(\mathbb{E} = 0) = 0.0001$$

$$\tilde{\alpha} = \begin{cases} 0, & \text{if } \alpha < \alpha_{\min} \\ \alpha, & \text{if } \alpha_{\min} \leq \alpha \leq 1 - \alpha_{\min} \\ 1, & \text{if } 1 - \alpha_{\min} < \alpha \end{cases}$$

$$\alpha^{\text{final}} = \max_{e \in V_e} \{\alpha, 0.5 \alpha_e\}$$

Choosing β_1, β_2

$$\mathbb{E} = \max \left(\frac{m_{N+1}^2}{\beta_1 m_1 + \sum_{j=2}^{N+1} m_j^2}, \frac{m_N^2}{\beta_2 m_1 + \sum_{j=2}^N m_j^2} \right)$$

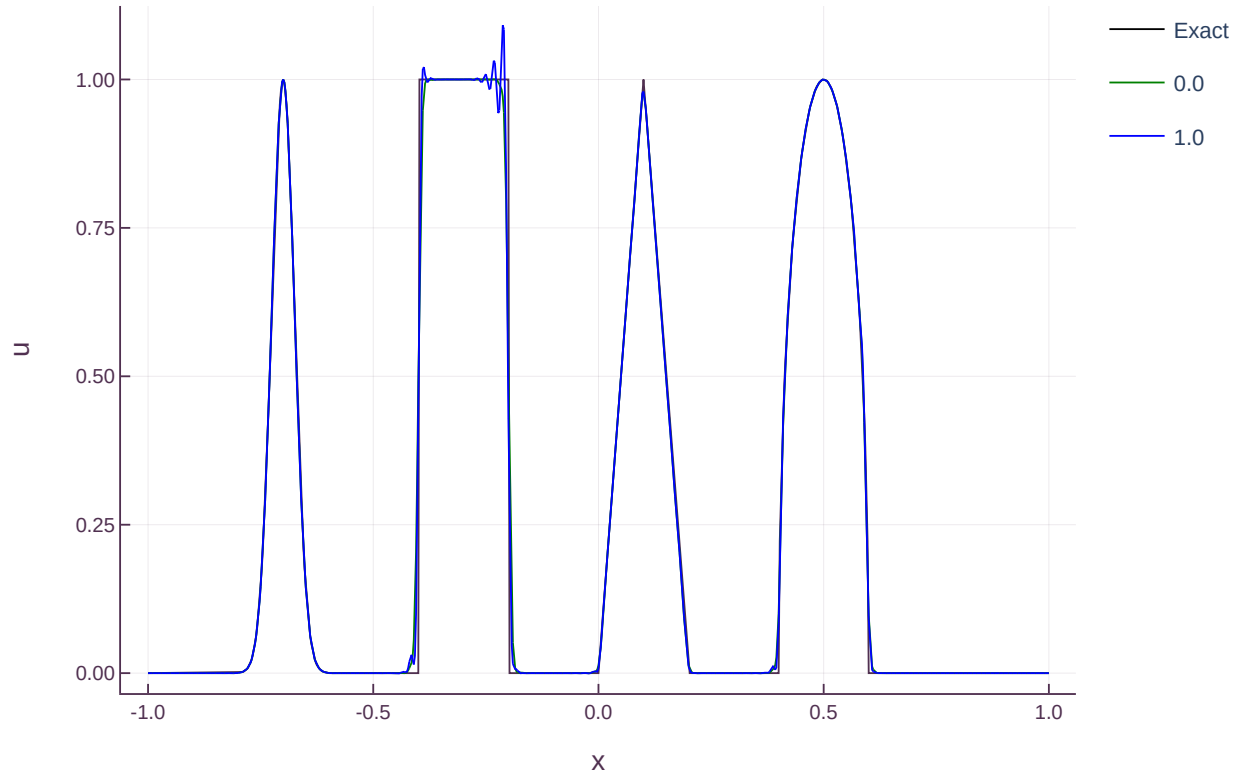


Figure 1. Comparing $\beta_1 = 0$ and $\beta_1 = 1$. β_2 has been set to 1.

Choosing β_1, β_2

$$\mathbb{E} = \max \left(\frac{m_{N+1}^2}{\beta_1 m_1 + \sum_{j=2}^{N+1} m_j^2}, \frac{m_N^2}{\beta_2 m_1 + \sum_{j=2}^N m_j^2} \right)$$

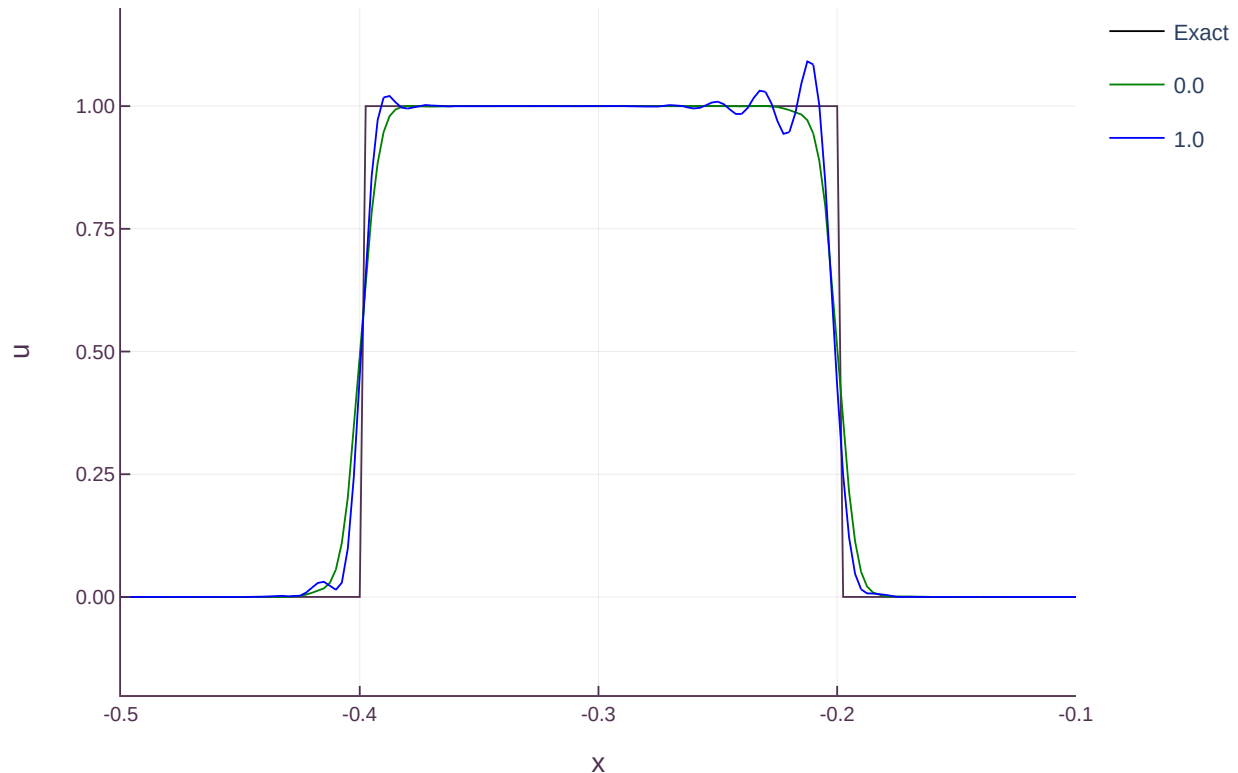


Figure 2. Comparing $\beta_1 = 0$ and $\beta_1 = 1$. β_2 has been set to 1.

Choosing β_1, β_2

$$\mathbb{E} = \max \left(\frac{m_{N+1}^2}{\beta_1 m_1 + \sum_{j=2}^{N+1} m_j^2}, \frac{m_N^2}{\beta_2 m_1 + \sum_{j=2}^N m_j^2} \right)$$

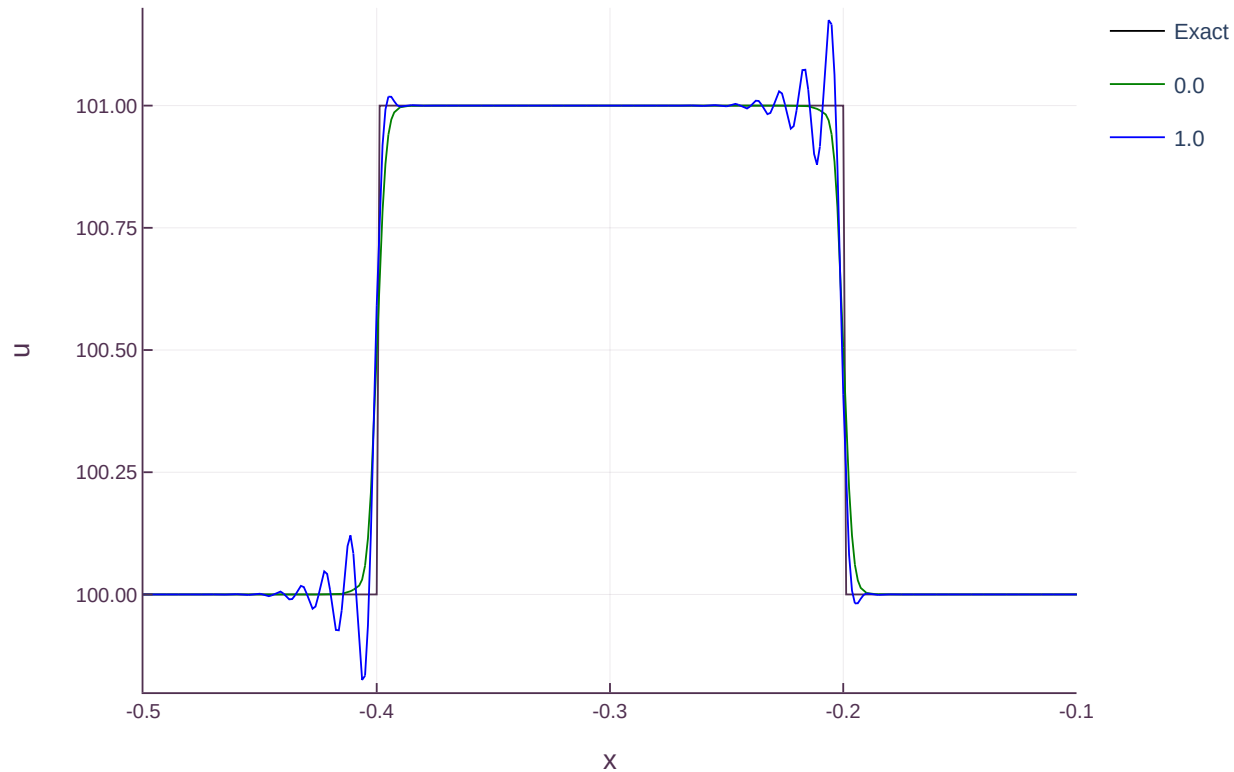


Figure 3. Comparing $\beta_1 = 0$ and $\beta_1 = 1$. β_2 has been set to 1.

Lower order update

Solution points and subcells



In the physical cell $I_e = [x_{e-\frac{1}{2}}, x_{e+\frac{1}{2}}]$, we define subcells $\left\{ \left[x_{j-\frac{1}{2}}^e, x_{j+\frac{1}{2}}^e \right] \right\}_{j:1}^{N+1}$ with (sub)faces $x_{j+\frac{1}{2}}^e$ defined as

$$x_{j+\frac{1}{2}}^e = x_{e-\frac{1}{2}} + \Delta x_e \sum_{1 \leq k \leq j} w_k, \quad 0 \leq j \leq N+1,$$

where $\{w_j\}_{j:1}^{N+1}$ are the Gauss-Legendre quadrature weights.

With this, we can define the lower order update in subcells to be

$$\begin{aligned} (u_1^e)^{n+1} &= (u_1^e)^n - \frac{\Delta t}{w_0 \Delta x_e} \left[f_{\frac{3}{2}} - F_{e-\frac{1}{2}}^L \right], \\ (u_j^e)^{n+1} &= (u_j^e)^n - \frac{\Delta t}{w_j \Delta x_e} \left[f_{j+\frac{1}{2}} - f_{j-\frac{1}{2}} \right], \quad 2 \leq j \leq N, \\ (u_N^e)^{n+1} &= (u_N^e)^n - \frac{\Delta t}{w_{N+1} \Delta x_e} \left[F_{e+\frac{1}{2}}^L - f_{N-\frac{1}{2}} \right]. \end{aligned} \tag{1}$$

Multiply j^{th} equation in (1) by w_j to get

$$\begin{aligned} \sum_{j:1}^{N+1} u_j^{L,n+1} w_j &= \sum_{j:1}^{N+1} u_j^e w_j - \frac{\Delta t}{\Delta x_e} (F_{e+1/2}^L - F_{e-1/2}^L) \\ \Rightarrow \bar{u}_e^{L,n+1} &= \bar{u}_e^{L,n} - \frac{\Delta t}{\Delta x_e} (F_{e+1/2}^L - F_{e-1/2}^L). \end{aligned}$$

Interface numerical flux

For LWFR, high order numerical flux $F_{e+\frac{1}{2}}^H$ is computed by time averaging and satisfies the conservation property

$$\bar{u}_e^{H,n+1} = \bar{u}_e^n - \frac{\Delta t}{\Delta x_e} \left(F_{e+\frac{1}{2}}^H - F_{e-\frac{1}{2}}^H \right)$$

The same is true for the lower order method

$$\bar{u}_e^{L,n+1} = (\bar{u}^e)^n - \frac{\Delta t}{\Delta x_e} \left(F_{e+\frac{1}{2}}^L - F_{e-\frac{1}{2}}^L \right).$$

Thus, the blended update is given by

$$\bar{u}_e^{n+1} = \bar{u}_e^n - \Delta t \left(F_{e+\frac{1}{2}} - F_{e-\frac{1}{2}} \right),$$

$$\text{where } F_{e+\frac{1}{2}} = \alpha_e F_{e+\frac{1}{2}}^L + (1 - \alpha_e) F_{e+\frac{1}{2}}^H.$$

For conservation, we must have

$$\alpha_e F_{e+\frac{1}{2}}^L + (1 - \alpha_e) F_{e+\frac{1}{2}}^H = \alpha_{e+1} F_{e+\frac{1}{2}}^L + (1 - \alpha_{e+1}) F_{e+\frac{1}{2}}^H$$

$$\Rightarrow F_{e+\frac{1}{2}}^L = F_{e+\frac{1}{2}}^H$$

Interface numerical flux

Initial candidate for the interface flux :

$$\tilde{\mathbf{F}}_{e+\frac{1}{2}} = \left(1 - \alpha_{e+\frac{1}{2}}\right) \mathbf{F}_{e+\frac{1}{2}}^{\text{LW}_1} + \alpha_{e+\frac{1}{2}} \mathbf{f}_{e,N+3/2}, \quad \alpha_{e+\frac{1}{2}} = \frac{1}{2}(\alpha_e + \alpha_{e+1}).$$

Then the lower order update of last solution point would be

$$\tilde{\mathbf{u}}^{n+1} = \mathbf{u}_{e,N+1}^n - \frac{\Delta t}{\Delta x_e w_{N+1}} (\tilde{\mathbf{F}}_{e+\frac{1}{2}} - \mathbf{f}_{e,N+1/2}).$$

Assume there is a **concave** p such that the admissibility condition $\mathbf{u} \in \Omega$ is equivalent to

$$p(\mathbf{u}) > 0.$$

Our lower order method is chosen so that

$$\tilde{\mathbf{u}}_{\text{low}}^{n+1} = \mathbf{u}_{e,N+1}^n - \frac{\Delta t}{\Delta x_e w_{N+1}} (\mathbf{f}_{e,N+3/2} - \mathbf{f}_{e,N+1/2}) \in \Omega.$$

Thus, for

$$\theta = \min \left(\left| \frac{\epsilon - p(\tilde{\mathbf{u}}_{\text{low}}^{n+1})}{p(\tilde{\mathbf{u}}^{n+1}) - p(\tilde{\mathbf{u}}_{\text{low}}^{n+1})} \right|, 1 \right),$$

we will have

$$p(\theta \tilde{\mathbf{u}}^{n+1} + (1 - \theta) \mathbf{u}_{\text{low}}^{n+1}) > \epsilon.$$

Finally choose

$$\mathbf{F}_{e+\frac{1}{2}} = \theta \tilde{\mathbf{F}}_{e+\frac{1}{2}} + (1 - \theta) \mathbf{f}_{e,N+3/2}.$$

Extension of Zhang-Shu's limiter to Lax-Wendroff schemes

Recall that the lower order update looks like

$$\begin{aligned}(\tilde{\mathbf{u}}_1^e)^{n+1} &= (\mathbf{u}_1^e)^n - \frac{\Delta t}{w_0 \Delta x_e} \left[f_{\frac{3}{2}} - F_{e-\frac{1}{2}} \right], \\ (\tilde{\mathbf{u}}_j^e)^{n+1} &= (\mathbf{u}_j^e)^n - \frac{\Delta t}{w_j \Delta x_e} \left[f_{j+\frac{1}{2}} - f_{j-\frac{1}{2}} \right], \quad 2 \leq j \leq N, \\ (\tilde{\mathbf{u}}_N^e)^{n+1} &= (\mathbf{u}_N^e)^n - \frac{\Delta t}{w_{N+1} \Delta x_e} \left[F_{e+\frac{1}{2}} - f_{N-\frac{1}{2}} \right].\end{aligned}$$

With our choice of $F_{e \pm \frac{1}{2}}$, we have

$$\tilde{\mathbf{u}}_j^e \in \Omega, \quad 1 \leq j \leq N+1.$$

This gives us

$$\bar{\mathbf{u}}_e^{n+1} = \bar{\mathbf{u}}_e^n - \frac{\Delta t}{\Delta x_e} \left(F_{e+\frac{1}{2}} - F_{e-\frac{1}{2}} \right) = \sum_{j=1}^{N+1} w_j \tilde{\mathbf{u}}_j^{n+1} \in \Omega.$$

Thus, the cell averages preserve admissibility and we can now use Zhang-Shu's admissibility preserving limiter to obtain an admissibility preserving Lax-Wendroff scheme.

The approach of preserving admissibility of cell averages and using Zhang-Shu's limiter has also been explored by Rossmanith Et Al. [3]. The advantage of our proposed approach over theirs is that we don't require additional cell/face loops and there are very little (and optional) additional storage requirements.

Now that our lower order method is admissibility preserving, we can also aposteriorily modify α_e to ensure that the blended scheme is admissibility preserving. This approach has been explored by Gassner and Ramírez in [13].

Admissibility preservation in 2-D

$$\begin{aligned} \text{Initial candidate: } \tilde{F}_{e_x+\frac{1}{2}, e_y, j} &= (1 - \alpha_{e_x+\frac{1}{2}, e_y}) F_{e_x+\frac{1}{2}, e_y, j}^{\text{LW}} + \alpha_{e_x+\frac{1}{2}, e_y} f_{\mathbf{e}, N+\frac{3}{2}, j}, & 1 \leq j \leq N+1, \\ \tilde{F}_{e_x, e_y+\frac{1}{2}, i} &= (1 - \alpha_{e_x, e_y+\frac{1}{2}}) F_{e_x, e_y+\frac{1}{2}, i}^{\text{LW}} + \alpha_{e_x, e_y+\frac{1}{2}} f_{\mathbf{e}, i, N+\frac{3}{2}}, & 1 \leq i \leq N+1. \end{aligned}$$

$$\begin{aligned} \tilde{\mathbf{u}}^{n+1} &= \mathbf{u}_{\mathbf{e}, 1, j}^n - \frac{\Delta t}{\Delta x_{\mathbf{e}} w_1} \left(\tilde{F}_{e_x+\frac{1}{2}, e_y, j} - f_{\mathbf{e}, \frac{1}{2}, j} \right) - \frac{\Delta t}{\Delta y_{\mathbf{e}} w_j} \left(f_{\mathbf{e}, 1, j+\frac{1}{2}} - f_{\mathbf{e}, 1, j-\frac{1}{2}} \right), \quad 1 < j < N+1, \\ \tilde{\mathbf{u}}^{n+1} &= \mathbf{u}_{\mathbf{e}, 1, 1}^n - \frac{\Delta t}{\Delta x_{\mathbf{e}} w_1} \left(\tilde{F}_{e_x+\frac{1}{2}, e_y, 1} - f_{\mathbf{e}, \frac{1}{2}, 1} \right) - \frac{\Delta t}{\Delta y_{\mathbf{e}} w_1} \left(\tilde{F}_{e_x, e_y+\frac{1}{2}, 1} - f_{\mathbf{e}, 1, \frac{1}{2}} \right), \quad j = 1. \end{aligned}$$

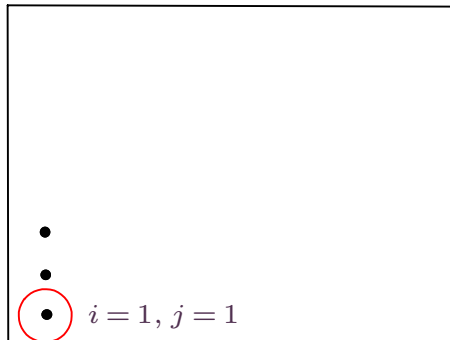
In the 2-D code, there's two separate face loops for vertical and horizontal faces. This poses a challenge because to ensure $\tilde{\mathbf{u}}^{n+1}$ is admissible, we need to correct both $\tilde{F}_{e_x+\frac{1}{2}, e_y, 1}$ and $\tilde{F}_{e_x, e_y+\frac{1}{2}, 1}$ and these values are never available together.

To avoid having to store values and doing aposteriori correction, we find appropriate λ_x, λ_y such that

$$\lambda_x + \lambda_y = 1,$$

and then, following the 1-D procedure, construct corrected $F_{e_x+\frac{1}{2}, e_y, 1}$ and $F_{e_x, e_y+\frac{1}{2}, 1}$ such that

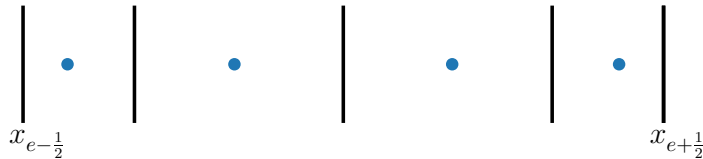
$$\begin{aligned} \mathbf{u}_{\mathbf{e}, 1, 1}^n - \frac{\Delta t}{\Delta x_{\mathbf{e}} \lambda_x w_1} \left(\tilde{F}_{e_x+\frac{1}{2}, e_y, 1} - f_{\mathbf{e}, \frac{1}{2}, 1} \right) &\in \Omega, \\ \mathbf{u}_{\mathbf{e}, 1, 1}^n - \frac{\Delta t}{\Delta y_{\mathbf{e}} \lambda_y w_1} \left(\tilde{F}_{e_x, e_y+\frac{1}{2}, 1} - f_{\mathbf{e}, 1, \frac{1}{2}} \right) &\in \Omega. \end{aligned}$$



$$\lambda_x = \frac{|s_x^{\mathbf{e}}| / \Delta x_{\mathbf{e}}}{|s_x^{\mathbf{e}}| / \Delta x_{\mathbf{e}} + |s_y^{\mathbf{e}}| / \Delta y_{\mathbf{e}}}, \quad \lambda_y = \frac{|s_y^{\mathbf{e}}| / \Delta y_{\mathbf{e}}}{|s_x^{\mathbf{e}}| / \Delta x_{\mathbf{e}} + |s_y^{\mathbf{e}}| / \Delta y_{\mathbf{e}}}$$

Low order residual : MUSCL-Hancock

Solution points and subcells



Integrating the conservation law over the subcell I_j^e , we get

$$\Delta x_e w_j (\mathbf{u}_j^{n+1} - \mathbf{u}_j^n) + \int_{t^n}^{t^{n+1}} (\mathbf{f}_{j+1/2} - \mathbf{f}_{j-1/2}) dt = 0.$$

Using the mid-point rule, writing explicit update,

$$\mathbf{u}_j^{n+1} = \mathbf{u}_j^n - \frac{\Delta t}{\Delta x_e w_j} (\mathbf{f}_{j+1/2}^{n+1/2} - \mathbf{f}_{j-1/2}^{n+1/2})$$

$$\mathbf{f}_{j+1/2}^{n+1/2} = \mathbf{f}(\mathbf{u}_{j+1/2-}^{n+1/2}, \mathbf{u}_{j+1/2+}^{n+1/2})$$

$$\begin{aligned} \mathbf{u}_{j-1/2+} &= \mathbf{u}_j(x_{j-1/2}), & \mathbf{u}_{j+1/2-} &= \mathbf{u}_j(x_{j+1/2}) \\ \mathbf{u}_j(x) &= \mathbf{u}_j^n + \delta_j(x - x_j) \end{aligned}$$

$$\begin{aligned} \delta_j &= \text{minmod}\left(\beta_j \frac{\mathbf{u}_{j+1} - \mathbf{u}_j}{x_{j+1} - x_j}, D_{\text{cent}}(\mathbf{u})_j, \beta_j \frac{\mathbf{u}_j^n - \mathbf{u}_{j-1}^n}{x_j - x_{j-1}} \right) \\ \beta_j &= 2 - \alpha_j \end{aligned}$$

$$\mathbf{u}_{j-\frac{1}{2}+}^{n+1/2} = \mathbf{u}_{j-1/2}^n - \frac{\Delta t}{2} \frac{f(\mathbf{u}_{j+1/2}) - f(\mathbf{u}_{j-1/2})}{x_{j+1/2} - x_{j-1/2}}, \quad \mathbf{u}_{j+\frac{1}{2}-}^{n+1/2} = \mathbf{u}_{j+1/2}^n - \frac{\Delta t}{2} \frac{f(\mathbf{u}_{j+1/2}) - f(\mathbf{u}_{j-1/2})}{x_{j+1/2} - x_{j-1/2}}.$$

Admissibility of low order method

Theorem 1. (*Extension of Berthon [1]*) Consider the conservation law

$$\mathbf{u}_t + \mathbf{f}(\mathbf{u})_x = 0$$

which preserves a convex set Ω . Let $\{\mathbf{u}_i^n\}_{i \in \mathbb{Z}}$ be the approximate solution at time level n and assume that $\mathbf{u}_i^n \in \Omega$ for all $i \in \mathbb{Z}$. Consider **conservative reconstructions**

$$\mathbf{u}_i^{n,+} = \mathbf{u}_i + (x_{i+1/2} - x_i) \boldsymbol{\sigma}_i, \quad \mathbf{u}_i^{n,-} = \mathbf{u}_i + (x_{i-1/2} - x_i) \boldsymbol{\sigma}_i.$$

Define $\mathbf{u}_i^{*,\pm}$ satisfying

$$\mu^- \mathbf{u}_i^{n,-} + \mathbf{u}_i^{*,\pm} + \mu^+ \mathbf{u}_i^{n,+} = 2\mathbf{u}_i^{n,\pm},$$

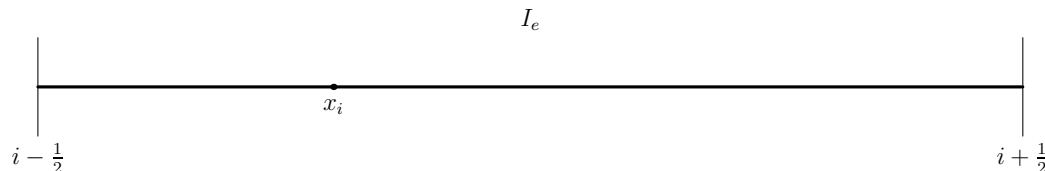
where

$$\mu^- = \frac{x_{i+1/2} - x_i}{x_{i+1/2} - x_{i-1/2}}, \quad \mu^+ = \frac{x_i - x_{i-1/2}}{x_{i+1/2} - x_{i-1/2}}.$$

Assume that the slope $\boldsymbol{\sigma}_i$ is chosen so that

$$\mathbf{u}_i^{*,\pm} \in \Omega.$$

Then, under **appropriate** time step restrictions, the updated solution \mathbf{u}_i^{n+1} , defined by the MUSCL-Hancock procedure is in Ω .



Generalizing Berthon's proof

Berthon defined $\mathbf{u}_i^{*,\pm}$ to be the quantity satisfying

$$\frac{1}{2}\mathbf{u}_i^{n,-} + \mathbf{u}_i^{*,\pm} + \frac{1}{2}\mathbf{u}_i^{n,+} = 2\mathbf{u}_i^{n,\pm}.$$

For non-cell centred grids, we generalize to

$$\mu^- \mathbf{u}_i^{n,-} + \mathbf{u}_i^{*,\pm} + \mu^+ \mathbf{u}_i^{n,+} = 2\mathbf{u}_i^{n,\pm},$$

where

$$\mu^- = \frac{x_{i+1/2} - x_i}{x_{i+1/2} - x_{i-1/2}}, \quad \mu^+ = \frac{x_i - x_{i-1/2}}{x_{i+1/2} - x_{i-1/2}}.$$

This choice was made to get the natural expression of $\mathbf{u}_i^{*,\pm}$ in the **conservative reconstruction case** -

$$\mathbf{u}_i^{*,\pm} = \mathbf{u}_i^n + 2(x_{i\pm 1/2} - x_i)\boldsymbol{\sigma}_i,$$

noting that

$$\mathbf{u}_i^{n,+} = \mathbf{u}_i + (x_{i+1/2} - x_i)\boldsymbol{\sigma}_i, \quad \mathbf{u}_i^{n,-} = \mathbf{u}_i + (x_{i-1/2} - x_i)\boldsymbol{\sigma}_i.$$

Step 1 : Evolution to $n + 1/2$

Lemma 2. (*Evolution*) Pick

$$\mu^- = \frac{x_{i+1/2} - x_i}{x_{i+1/2} - x_{i-1/2}}, \quad \mu^+ = \frac{x_i - x_{i-1/2}}{x_{i+1/2} - x_{i-1/2}},$$

so that

$$\frac{\mu^-}{2} \mathbf{u}_i^{n,-} + \frac{1}{2} \mathbf{u}_i^{*,\pm} + \frac{\mu^+}{2} \mathbf{u}_i^{n,+} = \mathbf{u}_i^{n,\pm}.$$

Then, assume that

$$\mathbf{u}_i^{n,\pm} \in \Omega \quad \text{and} \quad \mathbf{u}_i^{*,\pm} \in \Omega,$$

and the CFL restrictions

$$\begin{aligned} \frac{\Delta t / 2}{\mu^- \Delta x / 2} \max_{i \in \mathbb{Z}} (|\sigma_e(\mathbf{u}_i^{n,-}, \mathbf{u}_i^{*,\pm})|) &\leq \frac{1}{2}, \\ \frac{\Delta t / 2}{\mu^+ \Delta x / 2} \max_{i \in \mathbb{Z}} (|\sigma_e(\mathbf{u}_i^{*,\pm}, \mathbf{u}_i^{n,+})|) &\leq \frac{1}{2}, \end{aligned} \tag{2}$$

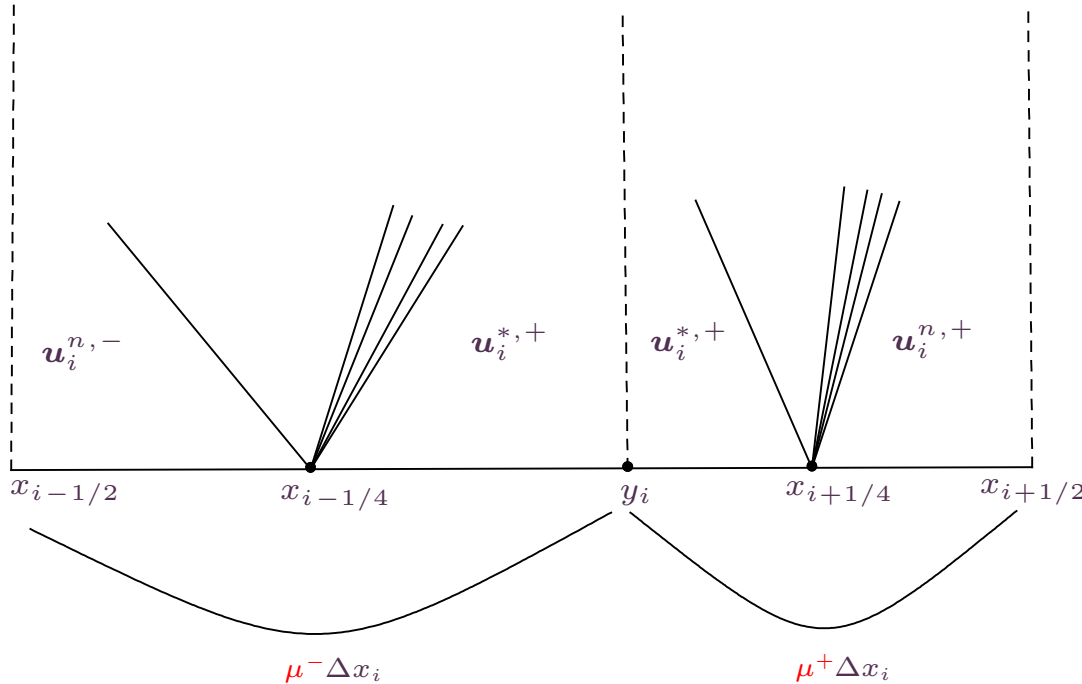
where $\sigma_e(\mathbf{u}_1, \mathbf{u}_2)$ denotes the maximum spectral radius among all Jacobian matrices at states between \mathbf{u}_1 and \mathbf{u}_2 .

Then, we have invariance of Ω under the first step of MUSCL-Hancock scheme, i.e.,

$$\mathbf{u}_i^{n+1/2,\pm} \in \Omega.$$

Step 1 : Evolution to $n + 1/2$

Proof



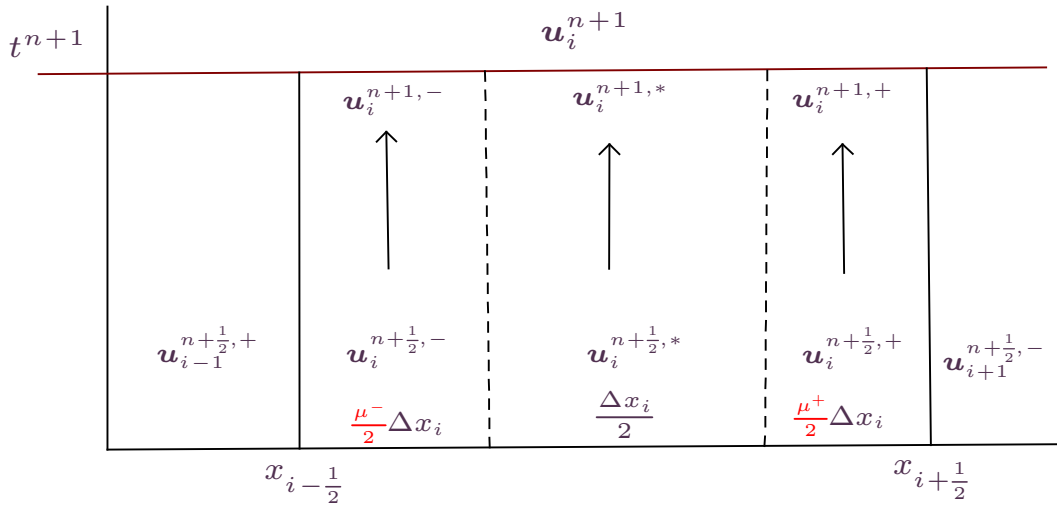
$$\begin{aligned}
 \tilde{\mathbf{u}}_i^{n+\frac{1}{2},+} &= \frac{1}{\Delta x_i} \int_{x_{i-1/2}}^{x_{i+1/2}} \mathbf{u}^h(x, \Delta t/2) dx \\
 &= \frac{1}{\Delta x_i} \left[\frac{y_i - x_{i-1/2}}{2} \mathbf{u}_i^{n,-} + \frac{\Delta x_i}{2} \mathbf{u}_i^{*,+} + \frac{x_{i+1/2} - y_i}{2} \mathbf{u}_i^{n,+} - \Delta t/2 (f(\mathbf{u}_i^{n,+}) - f(\mathbf{u}_i^{n,-})) \right] \\
 &= \frac{1}{2} (\mu^- \mathbf{u}_i^{n,-} + \mathbf{u}_i^{*,+} + \mu^+ \mathbf{u}_i^{n,+}) - \frac{\Delta t/2}{\Delta x_i} (f(\mathbf{u}_i^{n,+}) - f(\mathbf{u}_i^{n,-})) \\
 &= \mathbf{u}_i^{n,+} - \frac{\Delta t/2}{\Delta x_i} (f(\mathbf{u}_i^{n,+}) - f(\mathbf{u}_i^{n,-})) = \mathbf{u}_i^{n+\frac{1}{2},+}
 \end{aligned}$$

□

Step 2 : FVM type update

We introduce a new variable $\mathbf{u}_i^{n+\frac{1}{2}, *}$ defined so that

$$\mu^- \mathbf{u}_i^{n+\frac{1}{2}, -} + \mathbf{u}_i^{n+\frac{1}{2}, *} + \mu^+ \mathbf{u}_i^{n+\frac{1}{2}, +} = 2\mathbf{u}_i^n.$$



$$\mathbf{u}_i^{n+1, -} := \mathbf{u}_i^{n+\frac{1}{2}, -} - \frac{\Delta t}{\mu^- \Delta x_i / 2} \left(f\left(\mathbf{u}_i^{n+\frac{1}{2}, -}, \mathbf{u}_i^{n+\frac{1}{2}, *}\right) - f\left(\mathbf{u}_{i-1}^{n+\frac{1}{2}, +}, \mathbf{u}_i^{n+\frac{1}{2}, -}\right) \right)$$

$$\mathbf{u}_i^{n+1, *} := \mathbf{u}_i^{n+\frac{1}{2}, *} - \frac{\Delta t}{\Delta x_i / 2} \left(f\left(\mathbf{u}_i^{n+\frac{1}{2}, *}, \mathbf{u}_i^{n+\frac{1}{2}, +}\right) - f\left(\mathbf{u}_i^{n+\frac{1}{2}, -}, \mathbf{u}_i^{n+\frac{1}{2}, *}\right) \right)$$

$$\mathbf{u}_i^{n+1, +} := \mathbf{u}_i^{n+\frac{1}{2}, +} - \frac{\Delta t}{\mu^+ \Delta x_i / 2} \left(f\left(\mathbf{u}_i^{n+\frac{1}{2}, +}, \mathbf{u}_{i+1}^{n+\frac{1}{2}, -}\right) - f\left(\mathbf{u}_i^{n+\frac{1}{2}, *}, \mathbf{u}_i^{n+\frac{1}{2}, +}\right) \right)$$

$$\mathbf{u}_i^{n+1} = \mathbf{u}_i^n - \frac{\Delta t}{\Delta x} \left(f\left(\mathbf{u}_i^{n+\frac{1}{2}, +}, \mathbf{u}_{i+1}^{n+\frac{1}{2}, -}\right) - f\left(\mathbf{u}_{i-1}^{n+\frac{1}{2}, +}, \mathbf{u}_i^{n+\frac{1}{2}, -}\right) \right)$$

Step 2 : FVM type update

Lemma 3. (*Riemann solver*) Assume that the states $(\mathbf{u}_i^{n+\frac{1}{2}, \pm})_{i \in \mathbb{Z}}, (\mathbf{u}_i^{n+\frac{1}{2}, *})_{i \in \mathbb{Z}}$ belong to Ω , where $\mathbf{u}_i^{n+\frac{1}{2}, *}$ was defined above as

$$\mu^- \mathbf{u}_i^{n+\frac{1}{2}, -} + \mathbf{u}_i^{n+\frac{1}{2}, *} + \mu^+ \mathbf{u}_i^{n+\frac{1}{2}, +} = 2\mathbf{u}_i^n.$$

Then, the updated solution of MUSCL-Hancock scheme is in Ω under the CFL conditions

$$\begin{aligned}
 & \frac{\Delta t}{\mu^- \Delta x_i / 2} \max_{i \in \mathbb{Z}} \left(\left| \sigma_e \left(\mathbf{u}_i^{n+\frac{1}{2}, -}, \mathbf{u}_i^{n+\frac{1}{2}, *} \right) \right| \right) \leq \frac{1}{2}, \\
 & \frac{\Delta t}{\mu^- \Delta x_i / 2} \max_{i \in \mathbb{Z}} \left(\left| \sigma_e \left(\mathbf{u}_{i-1}^{n+\frac{1}{2}, +}, \mathbf{u}_i^{n+\frac{1}{2}, -} \right) \right| \right) \leq \frac{1}{2}, \\
 & \frac{\Delta t}{\Delta x_i / 2} \max_{i \in \mathbb{Z}} \left(\left| \sigma_e \left(\mathbf{u}_i^{n+\frac{1}{2}, *}, \mathbf{u}_i^{n+\frac{1}{2}, +} \right) \right| \right) \leq \frac{1}{2}, \\
 & \frac{\Delta t}{\Delta x_i / 2} \max_{i \in \mathbb{Z}} \left(\left| \sigma_e \left(\mathbf{u}_i^{n+\frac{1}{2}, -}, \mathbf{u}_i^{n+\frac{1}{2}, *} \right) \right| \right) \leq \frac{1}{2}, \\
 & \frac{\Delta t}{\mu^+ \Delta x_i / 2} \max_{i \in \mathbb{Z}} \left(\left| \sigma_e \left(\mathbf{u}_i^{n+\frac{1}{2}, +}, \mathbf{u}_{i+1}^{n+\frac{1}{2}, -} \right) \right| \right) \leq \frac{1}{2}, \\
 & \frac{\Delta t}{\mu^+ \Delta x_i / 2} \max_{i \in \mathbb{Z}} \left(\left| \sigma_e \left(\mathbf{u}_i^{n+\frac{1}{2}, *}, \mathbf{u}_i^{n+\frac{1}{2}, +} \right) \right| \right) \leq \frac{1}{2}.
 \end{aligned} \tag{3}$$

Final admissibility condition

$$\mu^- \mathbf{u}_i^{n+\frac{1}{2}, -} + \mathbf{u}_i^{n+\frac{1}{2}, *} + \mu^+ \mathbf{u}_i^{n+\frac{1}{2}, +} = 2\mathbf{u}_i^n$$

Lemma 4. (*Link previous lemmas*) Define $\mathbf{u}_i^{*,*}$ to satisfy

$$\mu^- \mathbf{u}_i^{n,-} + \mathbf{u}_i^{*,*} + \mu^+ \mathbf{u}_i^{n,+} = 2(2\mathbf{u}_i^n - (\mu^- \mathbf{u}_i^{n,-} + \mu^+ \mathbf{u}_i^{n,+})), \quad (4)$$

where, as defined before,

$$\mu^- = \frac{x_{i+1/2} - x_i}{x_{i+1/2} - x_{i-1/2}}, \quad \mu^+ = \frac{x_i - x_{i-1/2}}{x_{i+1/2} - x_{i-1/2}}.$$

Assume that $\mathbf{u}_i^{n,\pm}$ and $\mathbf{u}_i^{*,*}$ are in Ω . Consider the CFL conditions

$$\begin{aligned} \frac{\Delta t / 2}{\mu^- \Delta x / 2} \max_{i \in \mathbb{Z}} (|\sigma_e(\mathbf{u}_i^{*,*}, \mathbf{u}_i^{n,-})|) &\leq \frac{1}{2}, \\ \frac{\Delta t / 2}{\mu^+ \Delta x / 2} \max_{i \in \mathbb{Z}} (|\sigma_e(\mathbf{u}_i^{n,+}, \mathbf{u}_i^{*,*})|) &\leq \frac{1}{2}, \end{aligned} \quad (5)$$

then $\mathbf{u}_i^{n+\frac{1}{2},*} \in \Omega$.

Remark 5. For conservative reconstruction, we actually have $\mathbf{u}_i^{*,*} = \mathbf{u}_i$.

Final admissibility condition

$$\mathbf{u}_i^{n+\frac{1}{2}, *} = (2\mathbf{u}_i^n - (\mu^- \mathbf{u}_i^{n,-} + \mu^+ \mathbf{u}_i^{n,+})) - \frac{\Delta t}{2\Delta x} [(f(\mathbf{u}_i^{n,-}) - f(\mathbf{u}_i^{n,+}))]$$

Lemma 6. (*Link previous lemmas*) Define $\mathbf{u}_i^{*,*}$ to satisfy

$$\mu^- \mathbf{u}_i^{n,-} + \mathbf{u}_i^{*,*} + \mu^+ \mathbf{u}_i^{n,+} = 2(2\mathbf{u}_i^n - (\mu^- \mathbf{u}_i^{n,-} + \mu^+ \mathbf{u}_i^{n,+})), \quad (6)$$

where, as defined before,

$$\mu^- = \frac{x_{i+1/2} - x_i}{x_{i+1/2} - x_{i-1/2}}, \quad \mu^+ = \frac{x_i - x_{i-1/2}}{x_{i+1/2} - x_{i-1/2}}.$$

Assume that $\mathbf{u}_i^{n,\pm}$ and $\mathbf{u}_i^{*,*}$ are in Ω . Consider the CFL conditions

$$\begin{aligned} \frac{\Delta t / 2}{\mu^- \Delta x / 2} \max_{i \in \mathbb{Z}} (|\sigma_e(\mathbf{u}_i^{*,*}, \mathbf{u}_i^{n,-})|) &\leq \frac{1}{2}, \\ \frac{\Delta t / 2}{\mu^+ \Delta x / 2} \max_{i \in \mathbb{Z}} (|\sigma_e(\mathbf{u}_i^{n,+}, \mathbf{u}_i^{*,*})|) &\leq \frac{1}{2}, \end{aligned} \quad (7)$$

then $\mathbf{u}_i^{n+\frac{1}{2}, *} \in \Omega$.

Remark 7. For conservative reconstruction, we actually have $\mathbf{u}_i^{*,*} = \mathbf{u}_i$.

Final admissibility condition

$$\mathbf{u}_i^{n+\frac{1}{2}, *} = \left(\underbrace{2\mathbf{u}_i^n - (\mu^- \mathbf{u}_i^{n,-} + \mu^+ \mathbf{u}_i^{n,+})}_{\mathbf{u}_i^n} \right) - \frac{\Delta t}{2\Delta x} [(f(\mathbf{u}_i^{n,-}) - f(\mathbf{u}_i^{n,+}))]$$

Lemma 8. (*Link previous lemmas*) Define $\mathbf{u}_i^{*,*}$ to satisfy

$$\mu^- \mathbf{u}_i^{n,-} + \mathbf{u}_i^{*,*} + \mu^+ \mathbf{u}_i^{n,+} = 2(2\mathbf{u}_i^n - (\mu^- \mathbf{u}_i^{n,-} + \mu^+ \mathbf{u}_i^{n,+})), \quad (8)$$

where, as defined before,

$$\mu^- = \frac{x_{i+1/2} - x_i}{x_{i+1/2} - x_{i-1/2}}, \quad \mu^+ = \frac{x_i - x_{i-1/2}}{x_{i+1/2} - x_{i-1/2}}.$$

Assume that $\mathbf{u}_i^{n,\pm}$ and $\mathbf{u}_i^{*,*}$ are in Ω . Consider the CFL conditions

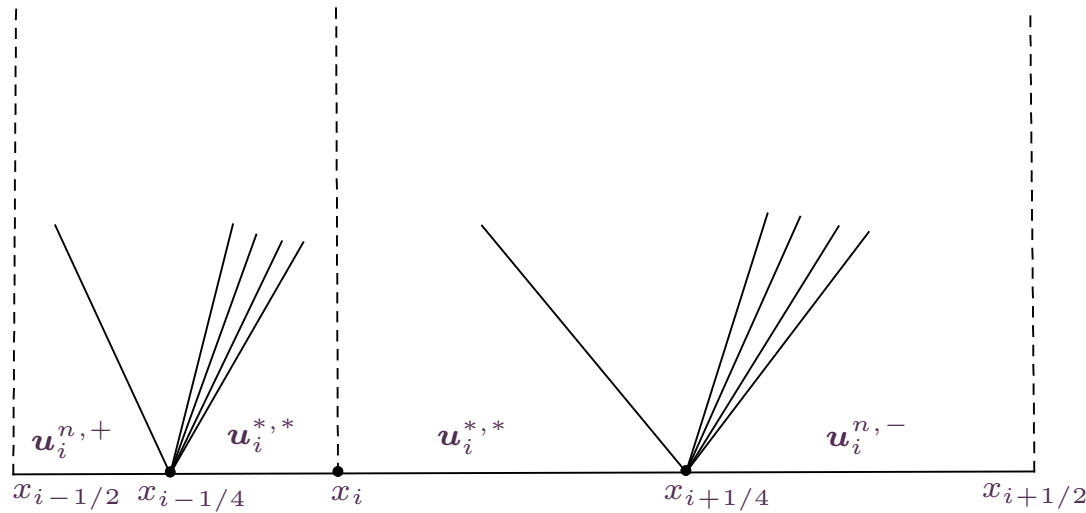
$$\begin{aligned} \frac{\Delta t / 2}{\mu^- \Delta x / 2} \max_{i \in \mathbb{Z}} (|\sigma_e(\mathbf{u}_i^{*,*}, \mathbf{u}_i^{n,-})|) &\leq \frac{1}{2}, \\ \frac{\Delta t / 2}{\mu^+ \Delta x / 2} \max_{i \in \mathbb{Z}} (|\sigma_e(\mathbf{u}_i^{n,+}, \mathbf{u}_i^{*,*})|) &\leq \frac{1}{2}, \end{aligned} \quad (9)$$

then $\mathbf{u}_i^{n+\frac{1}{2}, *} \in \Omega$.

Remark 9. For conservative reconstruction, we actually have $\mathbf{u}_i^{*,*} = \mathbf{u}_i$.

Final admissibility condition

Proof.



$$\begin{aligned}
 \tilde{\mathbf{u}}_i^{n+\frac{1}{2}, *} &= \frac{1}{\Delta x_i} \int_{x_{i-1/2}}^{x_{i+1/2}} \mathbf{u}^h \left(x, \frac{\Delta t}{2} \right) dx \\
 &= \frac{1}{\Delta x_i} \left(\frac{x_i - x_{i-1/2}}{2} \mathbf{u}_i^{n,+} + \frac{\Delta x_i}{2} \mathbf{u}_i^{*,*} + \frac{x_{i+1/2} - x_i}{2} \mathbf{u}_i^{n,-} - \frac{\Delta t}{2} (f(\mathbf{u}_i^{n,-}) - f(\mathbf{u}_i^{n,+})) \right) \\
 &= \frac{1}{2} (\mu^+ \mathbf{u}_i^{n,+} + \mathbf{u}_i^{*,*} + \mu^- \mathbf{u}_i^{n,-}) - \frac{\Delta t / 2}{\Delta x_i} (f(\mathbf{u}_i^{n,-}) - f(\mathbf{u}_i^{n,+})) \\
 &= \mathbf{u}_i^{n+\frac{1}{2}, *}
 \end{aligned}$$

Final admissibility condition

Theorem 10. Consider the conservation law

$$\mathbf{u}_t + \mathbf{f}(\mathbf{u})_x = 0$$

which preserves a convex set Ω . Let $\{\mathbf{u}_i^n\}_{i \in \mathbb{Z}}$ be the approximate solution at time level n and assume that $\mathbf{u}_i^n \in \Omega$ for all $i \in \mathbb{Z}$. Consider **conservative reconstructions**

$$\mathbf{u}_i^{n,+} = \mathbf{u}_i + (x_{i+1/2} - x_i) \boldsymbol{\sigma}_i, \quad \mathbf{u}_i^{n,-} = \mathbf{u}_i + (x_{i-1/2} - x_i) \boldsymbol{\sigma}_i.$$

Define $\mathbf{u}_i^{*,\pm}$ to be

$$\mathbf{u}_i^{*,\pm} = \mathbf{u}_i^n + 2\left(x_{i \pm \frac{1}{2}} - x_i\right) \boldsymbol{\sigma}_i$$

and assume that the slope σ_i is chosen so that

$$\mathbf{u}_i^{*,\pm} \in \Omega.$$

Then, under time step restrictions (2), (3), (9), the updated solution \mathbf{u}_i^{n+1} , defined by the MUSCL-Hancock procedure is in Ω .

Proof. We only need $\mathbf{u}_i^{n,\pm} \in \Omega$ to apply the previous lemmas. To that end, notice

$$\mathbf{u}_i^{n,\pm} = \frac{1}{2}\mathbf{u}_i^{*,\pm} + \frac{1}{2}\mathbf{u}_i^n.$$

□

Enforcing slope restriction

We are given that $\mathbf{u}_i^n \in \Omega$ and a candidate slope $\boldsymbol{\sigma}_i$. We have to limit it so that

$$\mathbf{u}_i^{*,\pm} = \mathbf{u}_i^n + 2(x_{i\pm 1/2} - x_i)\boldsymbol{\sigma}_i \in \Omega.$$

We shall do this by finding a $\theta \in [0, 1]$ such that

$$\mathbf{u}_i^n + \theta(2(x_{i\pm 1/2} - x_i)\boldsymbol{\sigma}_i) \in \Omega. \quad (10)$$

We assume that there is a concave function $p = p(\mathbf{u})$ such that the admissibility criterion is given by

$$p(\mathbf{u}) > 0.$$

We pick

$$\theta_{\pm} = \min \left(\left| \frac{\epsilon - p(\mathbf{u}_i^n)}{p(\mathbf{u}_i^{*,\pm}) - p(\mathbf{u}_i^n)} \right|, 1 \right)$$

and

$$\theta = \min(\theta_+, \theta_-).$$

By concavity of p ,

$$p(\theta \mathbf{u}_i^{*,\pm} + (1 - \theta) \mathbf{u}_i^n) > \theta p(\mathbf{u}_i^{*,\pm}) + (1 - \theta) p(\mathbf{u}_i^n) > \epsilon > 0.$$

Thus, this θ will give us (10). This approach is used when using Zhang-Shu's positivity limiter [20] in practice.

Non-conservative reconstruction

Consider non-conservative variables

$$\mathbf{U}_i^n = \kappa(\mathbf{u}_i^n),$$

so that reconstruction is given by

$$\mathbf{U}^n(x) = \mathbf{U}_i^n + \sigma_i(x - x_i)$$

$$\mathbf{u}_i^{n,\pm} := \kappa^{-1}(\mathbf{U}_i^{n,\pm}) \quad (11)$$

Theorem 11. Assume that $\mathbf{u}_i^n \in \Omega$ for all $i \in \mathbb{Z}$. Consider $\mathbf{u}_i^{n,\pm}$ defined in (11), $\mathbf{u}_i^{*,\pm}$ defined so that

$$\mu^- \mathbf{u}_i^{n+\frac{1}{2},-} + \mathbf{u}_i^{n+\frac{1}{2},*} + \mu^+ \mathbf{u}_i^{n+\frac{1}{2},+} = 2\mathbf{u}_i^n,$$

and $\mathbf{u}_i^{*,*}$ defined explicitly as

$$\mathbf{u}_i^{*,*} = 4\mathbf{u}_i^n - 3(\mu^- \mathbf{u}_i^{n,-} + \mu^+ \mathbf{u}_i^{n,+}).$$

Assume that the slope is chosen so that

$$\mathbf{u}_i^{n,\pm} \in \Omega, \quad \mathbf{u}_i^{*,\pm} \in \Omega \quad \text{and} \quad \mathbf{u}_i^{*,*} \in \Omega.$$

Consider the same CFL conditions (2), (3), (9). Then the updated solution \mathbf{u}_i^{n+1} of MUSCL-Hancock procedure is in Ω .

Remark 12. The definition of $\mathbf{u}_i^{*,*}$ comes from

$$\color{red}\mu^- \mathbf{u}_i^{n,-} + \mathbf{u}_i^{*,*} + \color{red}\mu^+ \mathbf{u}_i^{n,+} = 2(2\mathbf{u}_i^n - (\mu^- \mathbf{u}_i^{n,-} + \mu^+ \mathbf{u}_i^{n,+}))$$

ADER-DG : Predictor step

Current solution

$$x \in I_e: \quad u_h^n(\xi) = \sum_{j=1}^{N+1} u_j^n \ell_j(\xi)$$

Cell local space-time solution and flux: $\tau = (t - t_n) / \Delta t$

$$\tilde{u}_h(\xi, \tau) = \sum_{r,s=1}^{N+1} \tilde{u}_{rs} \ell_r(\xi) \ell_s(\tau), \quad \tilde{f}_h(\xi, \tau) = \sum_{r,s=1}^{N+1} f(\tilde{u}_{rs}) \ell_r(\xi) \ell_s(\tau).$$

Find \tilde{u}_h by cell local Galerkin method

$$\int_{t_n}^{t_{n+1}} \int_{I_e} (\partial_t \tilde{u}_h + \partial_x \tilde{f}_h) \ell_r(\xi) \ell_s(\tau) dx dt, \quad 1 \leq r, s \leq N+1.$$

Integrate by parts in time

$$\begin{aligned} & - \int_{t_n}^{t_{n+1}} \int_{I_e} \tilde{\mathbf{u}}_h \ell_r(\xi) \partial_t \ell_s(\tau) dx dt + \int_{I_e} \tilde{\mathbf{u}}_h(\xi, 1) \ell_r(\xi) \ell_s(1) dx - \int_{I_e} u_h^n(\xi) \ell_r(\xi) \ell_s(0) d\xi \\ & + \int_{t_n}^{t_{n+1}} \int_{I_e} \partial_x \tilde{f}_h \ell_r(\xi) \ell_s(\tau) dx dt = 0. \end{aligned}$$

ADER correction step

$$\int_{t_n}^{t_{n+1}} \int_0^1 (\partial_t u_h + \partial_x f(u_h)) \ell_i(\xi) dx dt = 0$$

Integrate by parts in space:

$$\begin{aligned} \int_{I_e} u_h^{n+1} \ell_i(\xi) dx &= \int_{I_e} u_h^n \ell_i(\xi) dx + \int_{t^n}^{t^{n+1}} \int_{I_e} \tilde{f}_h \partial_x \ell_i(\xi) dx dt \\ &\quad + \int_{t^n}^{t^{n+1}} f(\tilde{u}_{e-\frac{1}{2}}^-(t), \tilde{u}_{e-\frac{1}{2}}^+(t)) \ell_i(0) dt - \int_{t^n}^{t^{n+1}} f(\tilde{u}_{e+\frac{1}{2}}^-(t), \tilde{u}_{e+\frac{1}{2}}^+(t)) \ell_i(1) dt. \end{aligned}$$

Another integration by parts :

$$\begin{aligned} \int_{I_e} u_h^{n+1} \ell_i(\xi) dx &= \int_{I_e} u_h^n \ell_i(\xi) dx - \int_{t^n}^{t^{n+1}} \int_{I_e} \partial_x \tilde{f}_h \ell_i(\xi) dx dt \\ &\quad + \int_{t^n}^{t^{n+1}} \left(f(\tilde{u}_{e-\frac{1}{2}}^-(t), \tilde{u}_{e-\frac{1}{2}}^+(t)) - \tilde{f}_h(0, \tau) \right) \ell_i(0) dt \\ &\quad - \int_{t^n}^{t^{n+1}} \left(f(\tilde{u}_{e+\frac{1}{2}}^-(t), \tilde{u}_{e+\frac{1}{2}}^+(t)) - \tilde{f}_h(1, \tau) \right) \ell_i(1) dt, \end{aligned}$$

Quadrature on solution points :

$$\begin{aligned} u_i^n - \int_{t^n}^{t^{n+1}} \partial_x \tilde{f}_h(\xi_i, \tau) dt \\ \Rightarrow u_i^{n+1} = + \frac{\ell_i(0)}{w_i} \int_{t^n}^{t^{n+1}} f(\tilde{u}_{e-\frac{1}{2}}^-(t), \tilde{u}_{e-\frac{1}{2}}^+(t)) - \tilde{f}_h(0, \tau) dt \\ - \frac{\ell_i(1)}{w_i} \int_{t^n}^{t^{n+1}} f(\tilde{u}_{e+\frac{1}{2}}^-(t), \tilde{u}_{e+\frac{1}{2}}^+(t)) - \tilde{f}_h(1, \tau) dt \end{aligned}$$

ADER correction step

$$\int_{t_n}^{t_{n+1}} \int_0^1 (\partial_t u_h + \partial_x f(u_h)) \ell_i(\xi) dx dt = 0$$

Integrate by parts in space:

$$\begin{aligned} \int_{I_e} u_h^{n+1} \ell_i(\xi) dx &= \int_{I_e} u_h^n \ell_i(\xi) dx + \int_{t^n}^{t^{n+1}} \int_{I_e} \tilde{f}_h \partial_x \ell_i(\xi) dx dt \\ &\quad + \int_{t^n}^{t^{n+1}} f(\tilde{u}_{e-\frac{1}{2}}^-(t), \tilde{u}_{e-\frac{1}{2}}^+(t)) \ell_i(0) dt - \int_{t^n}^{t^{n+1}} f(\tilde{u}_{e+\frac{1}{2}}^-(t), \tilde{u}_{e+\frac{1}{2}}^+(t)) \ell_i(1) dt. \end{aligned}$$

Another integration by parts :

$$\begin{aligned} \int_{I_e} u_h^{n+1} \ell_i(\xi) dx &= \int_{I_e} u_h^n \ell_i(\xi) dx - \int_{t^n}^{t^{n+1}} \int_{I_e} \partial_x \tilde{f}_h \ell_i(\xi) dx dt \\ &\quad + \int_{t^n}^{t^{n+1}} \left(f(\tilde{u}_{e-\frac{1}{2}}^-(t), \tilde{u}_{e-\frac{1}{2}}^+(t)) - \tilde{f}_h(0, \tau) \right) \ell_i(0) dt \\ &\quad - \int_{t^n}^{t^{n+1}} \left(f(\tilde{u}_{e+\frac{1}{2}}^-(t), \tilde{u}_{e+\frac{1}{2}}^+(t)) - \tilde{f}_h(1, \tau) \right) \ell_i(1) dt, \end{aligned}$$

Quadrature on solution points :

$$\begin{aligned} u_i^n - \int_{t^n}^{t^{n+1}} \partial_x \tilde{f}_h(\xi_i, \tau) dt \\ \Rightarrow u_i^{n+1} = -g'_L(\xi_i) \int_{t^n}^{t^{n+1}} f(\tilde{u}_{e-\frac{1}{2}}^-(t), \tilde{u}_{e-\frac{1}{2}}^+(t)) - \tilde{f}_h(0, \tau) dt \\ - g'_R(\xi_i) \int_{t^n}^{t^{n+1}} f(\tilde{u}_{e+\frac{1}{2}}^-(t), \tilde{u}_{e+\frac{1}{2}}^+(t)) - \tilde{f}_h(1, \tau) dt \end{aligned}$$

ADER and LWFR for constant linear advection

For constant linear advection

$$u_t + u_x = 0,$$

the ADER update is given by

$$\begin{aligned} u_i^n - \partial_x \int_{t^n}^{t^{n+1}} \tilde{u}_h(\xi_i, \tau) dt \\ u_i^{n+1} = -g'_L(\xi_i) \left[f\left(\int_{t^n}^{t^{n+1}} \tilde{u}_{e-\frac{1}{2}}^-(t) dt, \int_{t^n}^{t^{n+1}} \tilde{u}_{e-\frac{1}{2}}^+(t) dt \right) - \int_{t^n}^{t^{n+1}} \tilde{u}_h(0, \tau) dt \right] \\ - g'_R(\xi_i) \left[f\left(\int_{t^n}^{t^{n+1}} \tilde{u}_{e+\frac{1}{2}}^-(t) dt, \int_{t^n}^{t^{n+1}} \tilde{u}_{e+\frac{1}{2}}^+(t) dt \right) - \int_{t^n}^{t^{n+1}} \tilde{u}_h(1, \tau) dt \right] \end{aligned} \quad (12)$$

The LWFR update is given by

$$u_i^{n+1} = u_i^n - \partial_x U_h(\xi_i) - g'_L(\xi_i) \left[f(U_{e-\frac{1}{2}}^-, U_{e-\frac{1}{2}}^+) - U_h(0) \right] - g'_R(\xi_i) \left[f(U_{e+\frac{1}{2}}^-, U_{e+\frac{1}{2}}^+) - U_h(1) \right], \quad (13)$$

where

$$\begin{aligned} U_h^n &= u + \frac{\Delta t}{2} u_t + \frac{\Delta t^2}{3!} u_{tt} + \cdots + \frac{\Delta t^N}{(N+1)!} \frac{\partial^N u}{\partial t^N} \\ &= u - \frac{\Delta t}{2} u_x + \frac{\Delta t^2}{3!} u_{xx} + \cdots + (-1)^N \frac{\Delta t^N}{(N+1)!} \frac{\partial^N u}{\partial x^N}. \end{aligned}$$

Equivalence of ADER-FR and LWFR for linear case

Theorem 13. *For the linear advection equation*

$$u_t + u_x = 0,$$

the Lax-Wendroff Flux Reconstruction scheme with D2 dissipation and ADER-FR scheme are equivalent.

Proof. Let $u_e^n = u_e^n(x)$ denote the solution polynomial at time level n in element e .

Then, $\tilde{u}_h(x, t) := u_e^n(x - (t - t^n))$ is a weak solution of the equation

$$\begin{aligned}\tilde{u}_t + \tilde{u}_x &= 0, & x \in [x_{e-1/2}, x_{e+1/2}], t \in (t_n, t_{n+1}], \\ \tilde{u}(x, t^n) &= u_e^n(x), & t = t_n.\end{aligned}$$

Since the predictor equation has a **unique** solution of degree N [7, 2], the specified \tilde{u}_h must be **the** predictor solution.

$$\begin{aligned}\tilde{u}_h(x, t) &= \tilde{u}_h(x, t^n) + (t - t^n) \frac{\partial}{\partial t} \tilde{u}_h(x, t^n) + \dots + \frac{(t - t^n)^N}{N!} \frac{\partial^N}{\partial t^N} \tilde{u}_h(x, t^n) \\ &= u^n(x) - (t - t^n) \frac{\partial}{\partial x} u^n(x) + \dots + (-1)^N \frac{(t - t^n)^N}{N!} \frac{\partial^N}{\partial x^N} u^n(x) \\ \Rightarrow \quad \frac{1}{\Delta t} \int_{t^n}^{t^{n+1}} \tilde{u}_h(x, t) dt &= u^n(x) - \frac{\Delta t}{2} \frac{\partial}{\partial x} u^n(x) + \dots + (-1)^N \frac{\Delta t^N}{(N+1)!} \frac{\partial^N}{\partial x^N} u^n dt, \\ \Rightarrow \quad \frac{1}{\Delta t} \int_{t^n}^{t^{n+1}} \tilde{u}_h(x, t) dt &= U_h^n(x)\end{aligned}$$

Thus, the ADER-update (12) and the LWFR-update (13) are the same. \square

Numerical verification of equivalence of ADER and LW-D2

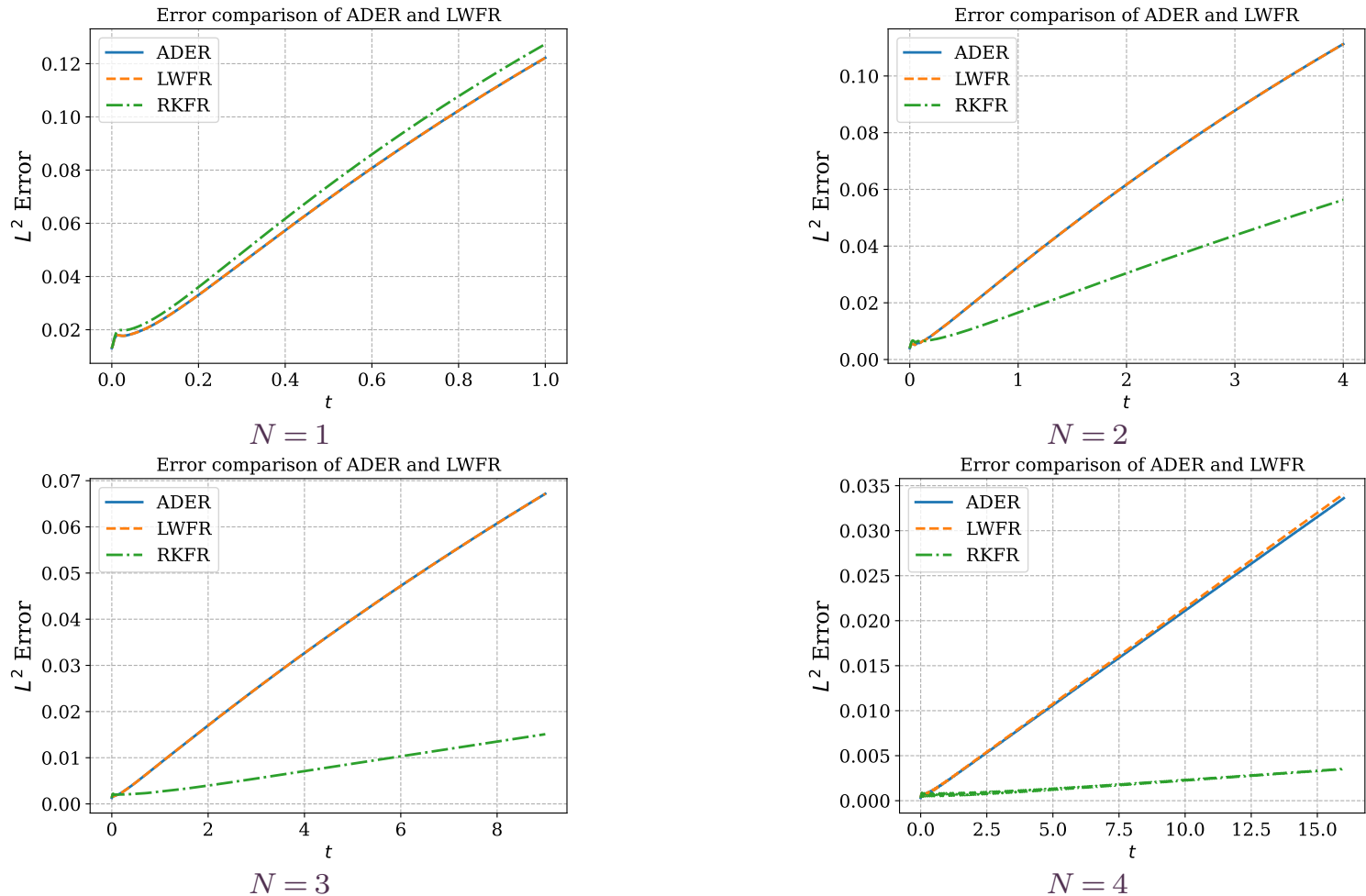
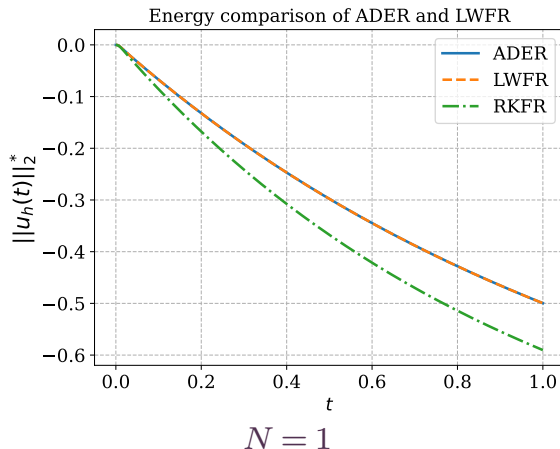


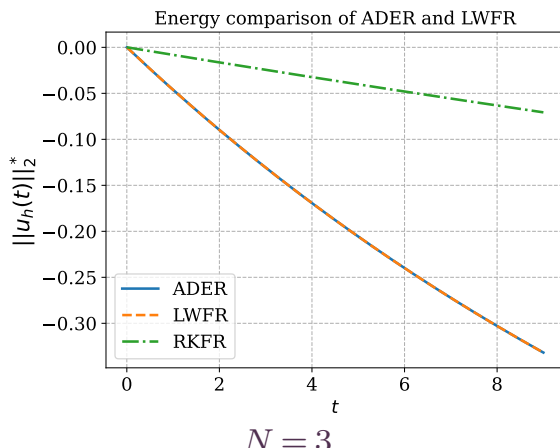
Figure 4. L^2 error comparison of ADER, LWFR and RKFR for linear advection equation with **wave packet** initial data $u_0(x) = e^{-10x^2} \sin(10\pi x)$ and **periodic boundary conditions** on $[-1, 1]$ with 120 degrees of freedom each.

Numerical verification of equivalence of ADER and LW-D2

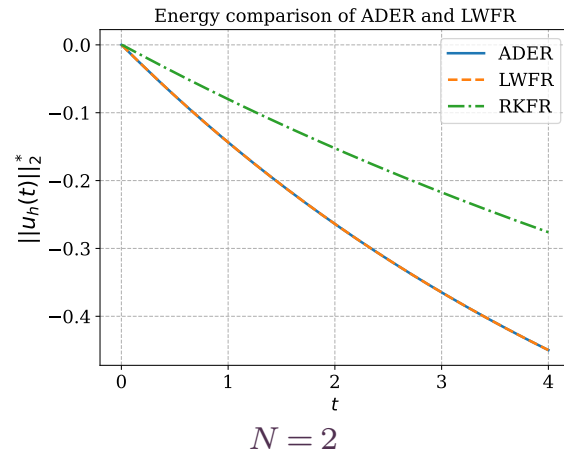
$$\|u(t)\|_2^* := \frac{\|u(t)\|_2 - \|u(0)\|_2}{\|u(0)\|_2}$$



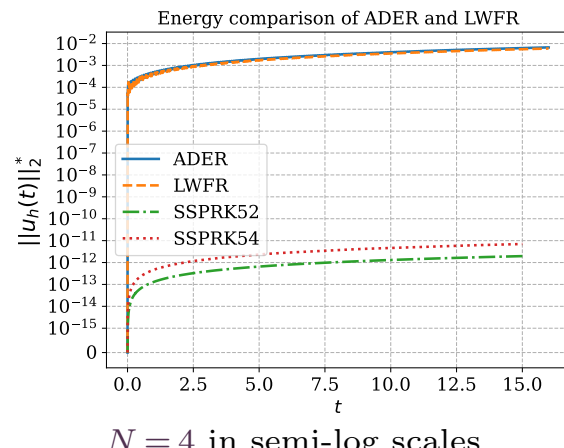
$N = 1$



$N = 3$



$N = 2$



$N = 4$ in semi-log scales

Figure 5. Energy comparison of ADER, LWFR and RKFR for linear advection equation with **smooth initial data** $u_0(x) = \sin(2\pi x)$ and **periodic boundary conditions** on $[-1, 1]$ with 120 degrees of freedom each.

ADER-FR and LWFR for non-linear case

Theorem 14. *If the predictor solution of ADER satisfies*

$$\|U^n\|_{C^{N+1}} \leq C$$

where C is a constant independent of $n, \Delta x, \Delta t$, then the ADER and LW solution will satisfy

$$\|u_{\text{ADER}}^{n+1} - u_{\text{LW}}^{n+1}\|_\infty = O(\Delta x^{N+1}).$$

Idea of proof. The weak formulation will give us

$$\tilde{u}_t + (\tilde{f}_h)_x = 0, \quad (14)$$

for all (x_r, t_s) where $s > 0$, i.e., $t_s > t^n$. Then, we can extrapolate to $t = t^n$ as

$$\tilde{u}_t + (\tilde{f}_h)_x = O(\Delta t^N) \quad \text{at } t = t^n,$$

so that we will have

$$\tilde{u}_h(x, t^n) = \tilde{u}_h(x, t^n) + \Delta t (\tilde{f}_h)_x + \dots + \frac{\Delta t^N}{N!} \frac{\partial^{N-1}}{\partial t^{N-1}} (\tilde{f}_h)_x + O(\Delta t^{N+1}).$$

Numerical Results

$$u_t+u_x=0$$

Convergence of pure MUSCL-Hancock method

$$\begin{aligned} u_t + u_x &= 0, & x \in [-1, 1], \quad t > 0, \\ u_0(x) &= \sin(2\pi x), & x \in [-1, 1]. \end{aligned}$$

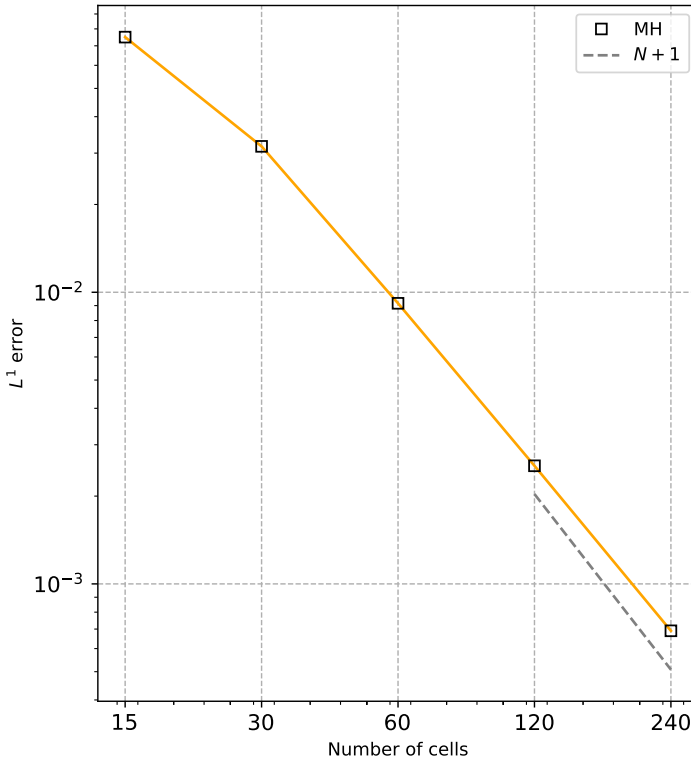


Figure 6. Convergence test of MUSCL-Hancock setting all $\alpha_e = 1$ showing close to second order convergence

Optimal convergence with limiter

$$\begin{aligned} u_t + u_x &= 0, & x \in [-2, 2], \quad t > 0, \\ u_0(x) &= e^{-10x^2} \sin(10\pi x), & x \in [-2, 2]. \end{aligned}$$

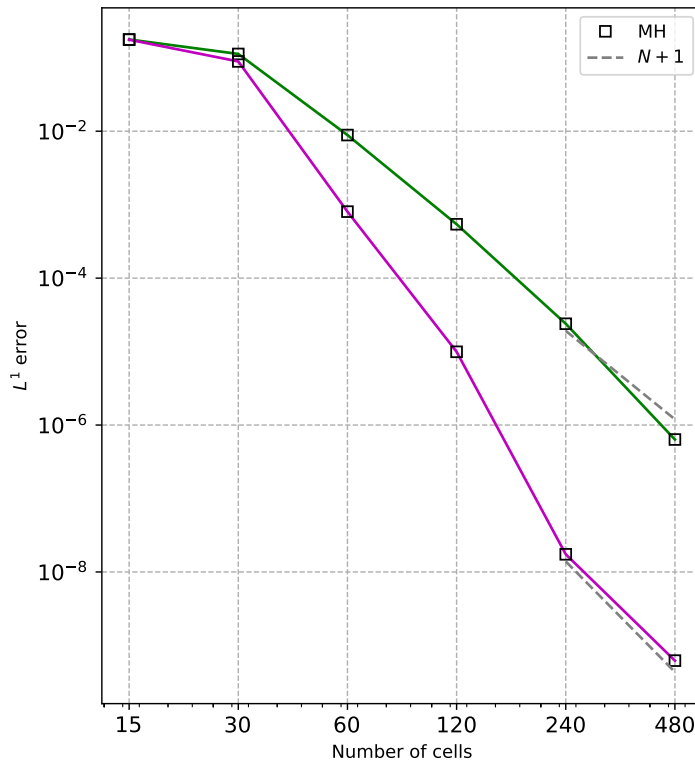


Figure 7. Convergence analysis with wave packet test case for $N = 3, 4$ at $t = 1$

Handling discontinuities

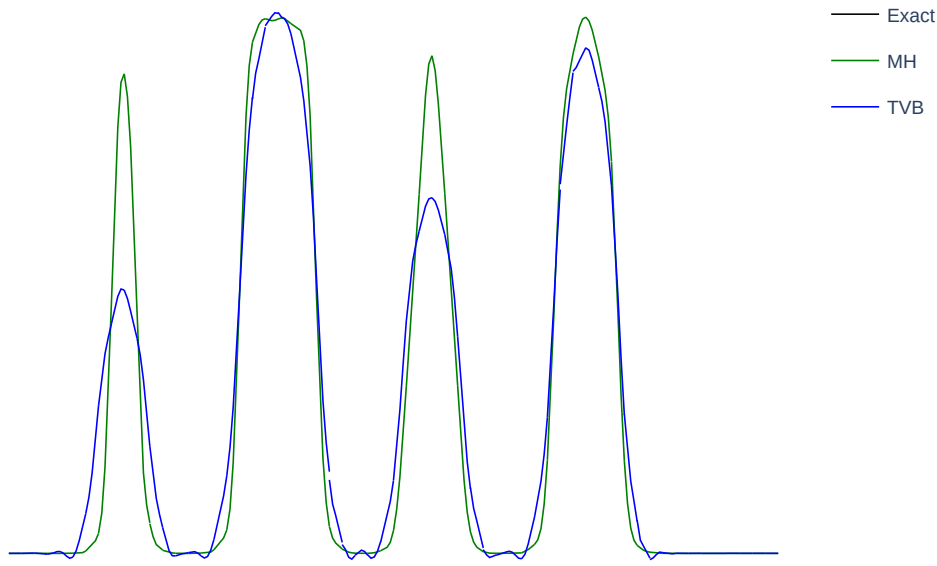


Figure 8. Composite signal [8] on a mesh of 60 cells for $N = 4$ comparing TVB limiter with parameter $M = 50$ and MUSCL-Hancock (MH) blending. Here, the smoothness indicator function has been set with $\beta_1 = 0.1$ and $\beta_2 = 1.0$.

$$\begin{aligned} u_t + u_x &= 0, & x \in [-1, 1], \quad t > 0, \\ u(x, 0) &= u_0(x), & x \in [-1, 1], \end{aligned}$$

$$u_0(x) = \begin{cases} G(x, \beta, z), & x \in [-0.8, 0.6], \\ 1, & x \in [-0.4, -0.2], \\ 1 - |10(x - 0.1)|, & x \in [0, 0.2], \\ F(x, \alpha, a), & x \in [0.4, 0.6], \\ 0, & \text{elsewhere}, \end{cases} \quad \begin{aligned} G(x, \beta, z) &= e^{-\beta(x-z)^2}, & F(x, \alpha, a) &= \sqrt{1 - \alpha^2(x-a)^2} \\ a &= 0.5, & z &= -0.7, & \delta &= 0.005, & \alpha &= 10, & \beta &= \frac{\log 2}{36 \delta^2}. \end{aligned}$$

1-D Euler's equations

$$\frac{\partial}{\partial t} \begin{pmatrix} \rho \\ \rho v \\ E \end{pmatrix} + \frac{\partial}{\partial x} \begin{pmatrix} \rho v \\ p + \rho v^2 \\ (E + p) v \end{pmatrix} = \mathbf{0}$$

where ρ , v , p and E denote the density, velocity, pressure and total energy of the gas, respectively. For a polytropic gas, an equation of state $E = E(\rho, v, p)$ which forms the system closed is given as

$$E = E(\rho, v, p) = \frac{p}{\gamma - 1} + \frac{1}{2} \rho v^2.$$

Shu-Osher

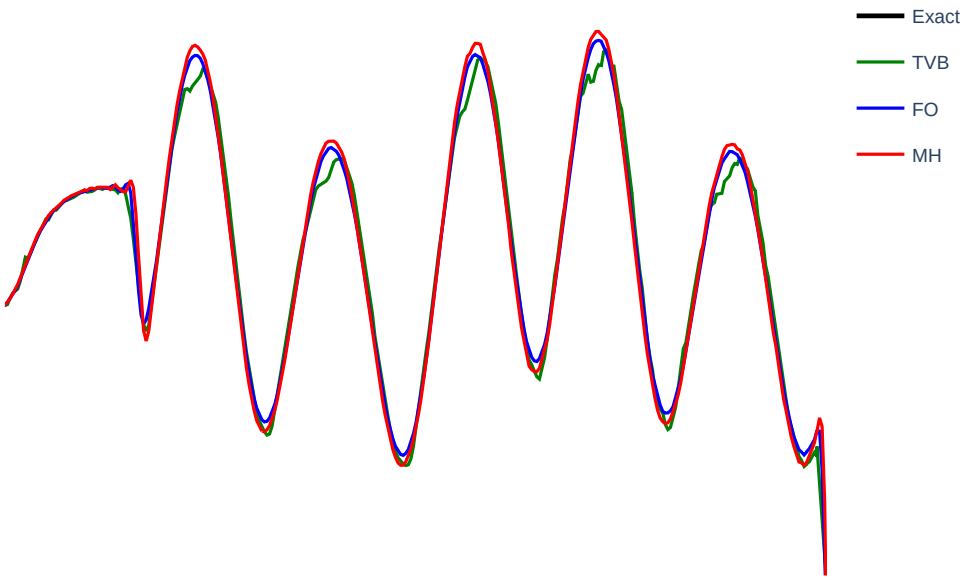


Figure 9. Density profile of Shu-Osher test case [16] at $t = 1.8$ for accuracy comparison of TVB limiter ($M = 300$, [12]), blending limiter with MUSCL-Hancock (MH) and First Order (FO) blending for degree $N = 4$ on a grid of 400 cells.

Transmissive boundary conditions on $[-5, 5]$ with

$$(\rho, v, p) = \begin{cases} (3.857143, 2.629369, 10.333333), & \text{if } x < -4, \\ (1 + 0.2 \sin(5x), 0, 1), & \text{if } x \geq -4, \end{cases}$$

and solution is plotted at $t = 1.8$.

Blast

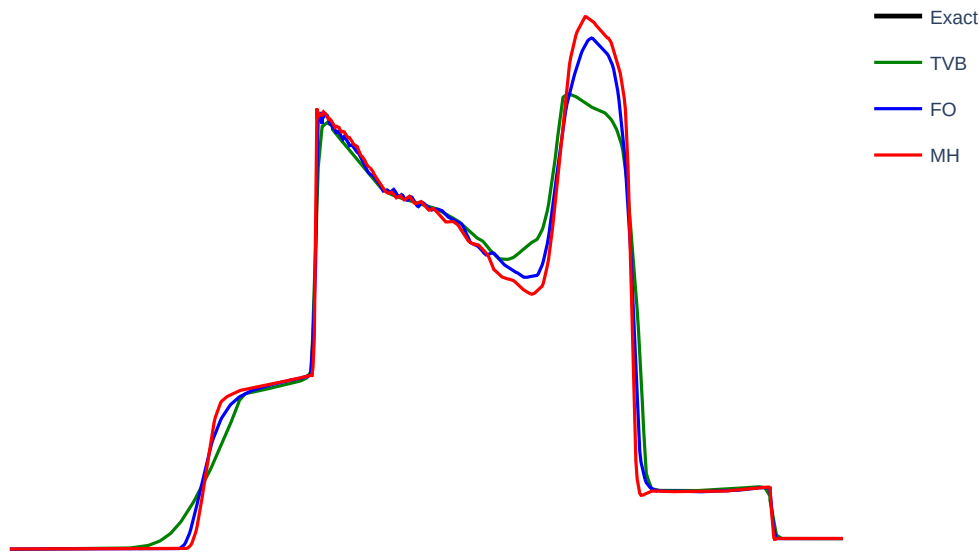


Figure 10. Density profile of Blast test of Woodward and Colella [18] for comparison of TVB limiter ($M = 300$, [12]), blending limiter with MUSCL-Hancock (MH) and First Order (FO) blending for degree $N = 4$ on a grid of 400 cells.

Solid wall boundary conditions on $[0, 1]$ with initial condition

$$(\rho, v, p) = \begin{cases} (1, 0, 1000), & \text{if } x < 0.1, \\ (1, 0, 0.01), & 0.1 < x < 0.9, \\ (1, 0, 100), & x > 0.9, \end{cases}$$

and solution is plotted at $t = 0.038$.

Sedov's blast wave

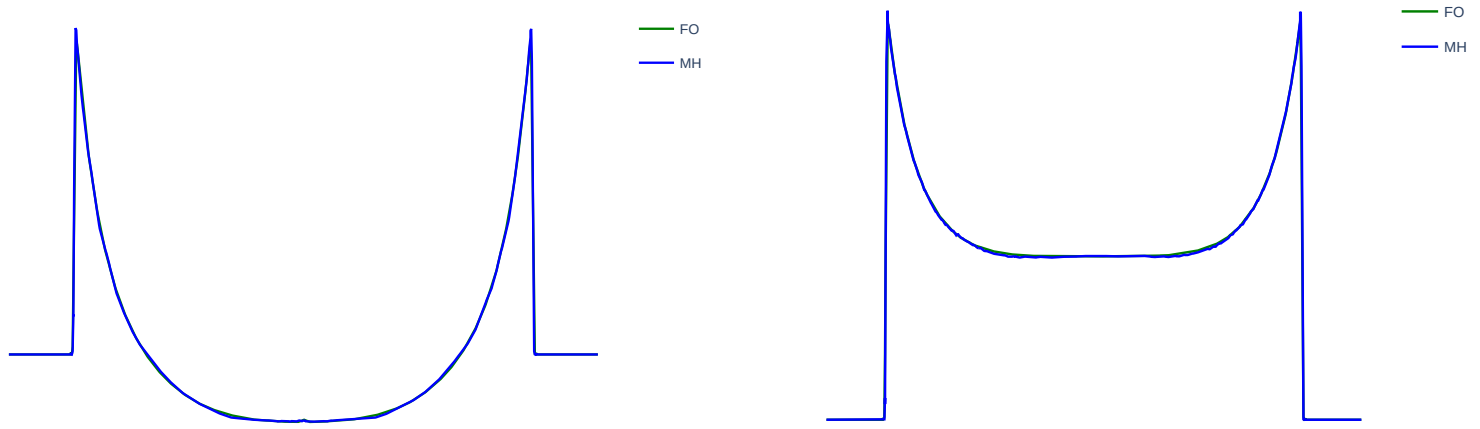


Figure 11. Density and pressure profiles of Sedov blast test case [15] on 201 elements for degree $N = 4$ to demonstrate admissibility preservation in very severe cases.

We impose transmissive boundary conditions on $[-1, 1]$ with number of elements $M_{\text{elem}} = 201$ and with the following intial data

$$\rho(x) = 1, \quad v(x) = 0, \quad p(x) = \begin{cases} (\gamma - 1) \frac{3.2 \times 10^6}{\Delta x}, & |x| \leq \frac{\Delta x}{2}, \\ (\gamma - 1) 10^{-12}, & \text{otherwise,} \end{cases}$$

where Δx is the mesh grid spacing. The odd number of elements are chosen so that the middle element

$$e = \frac{M_{\text{elem}} + 1}{2}$$

is centred at the origin. The solution is plotted at $t = 0.004$.

Double rarefaction

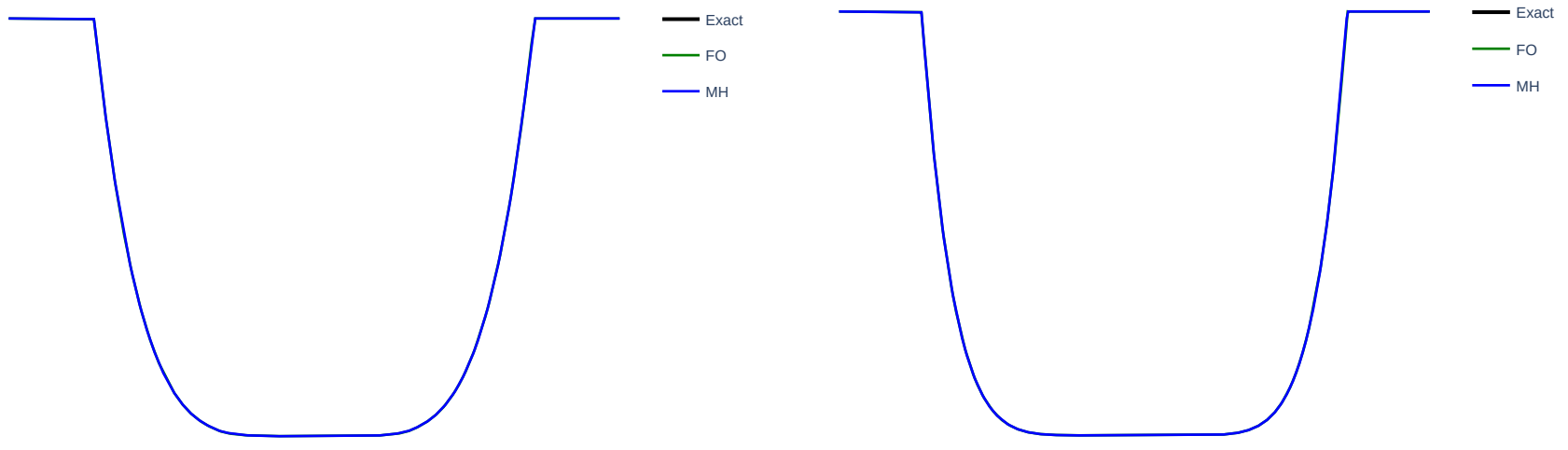


Figure 12. Density and pressure profiles of Double rarefaction test case of [10] on a mesh of 2000 elements for degree $N = 4$ to demonstrate admissibility preservation in a low density test case.

We impose transmissive boundary conditions on $[-1, 1]$ with initial conditions

$$(\rho, v, p) = \begin{cases} (7, -1, 0.2), & \text{if } x < 0, \\ (7, 1, 0.2), & \text{if } x > 0. \end{cases}$$

The solution is plotted at $t = 0.6$.

Leblanc's test

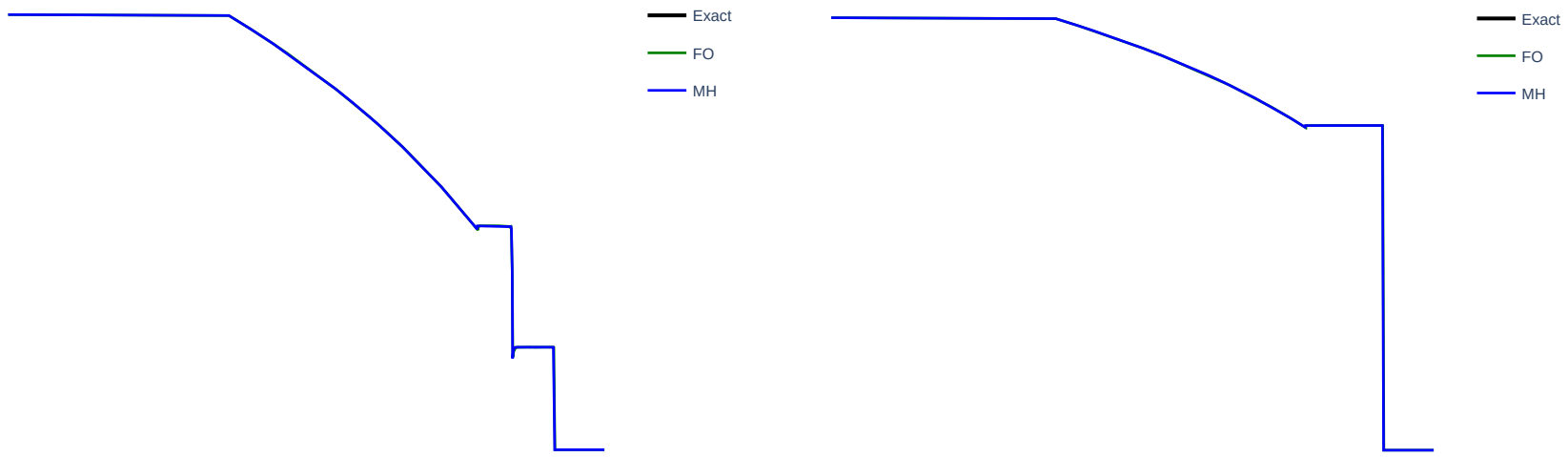


Figure 13. Density and pressure profiles of Leblanc test case on a mesh of 6400 elements for degree $N = 4$ to demonstrate admissibility preservation.

We impose transmissive boundary conditions on $[-10, 10]$ with initial conditions

$$(\rho, v, p) = \begin{cases} (2, 0, 10^9), & \text{if } x < 0, \\ (0.001, 0, 1), & \text{if } x > 0. \end{cases}$$

The solution is plotted at $t = 0.0001$.

2-D Results

2-D Composite signal [9]

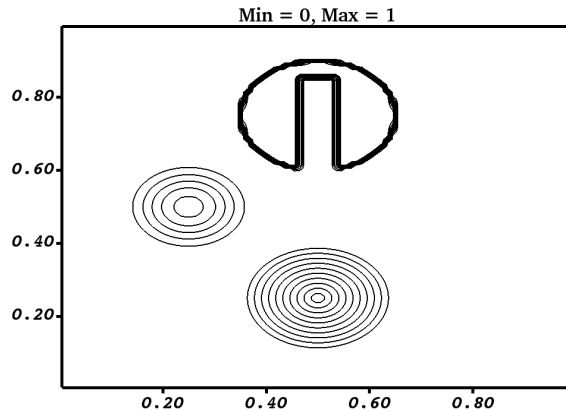


Figure 14. Initial data

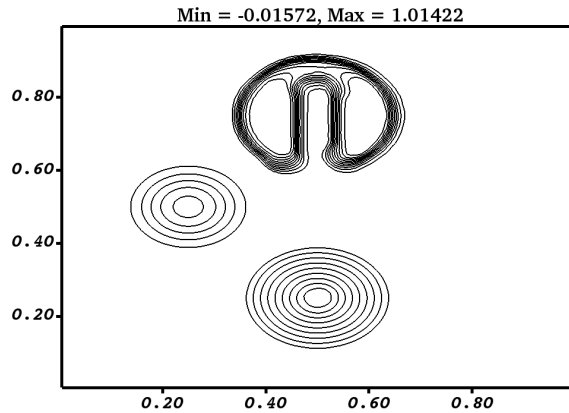


Figure 15. TVB with $M = 100$

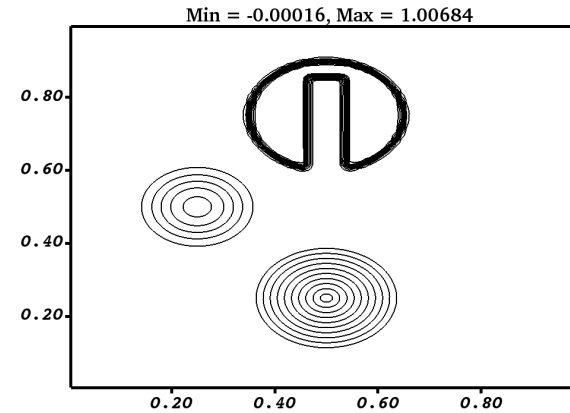


Figure 16. MUSCL-Hancock blending

We compare solutions on a 100×100 mesh with degree $N = 4$ at $t = 2\pi$ (1 period).

Double Mach Reflection



Figure 17. Density profile of Double Mach reflection [18] test case on a mesh of 568×142 cells using HLLC flux with MUSCL-Hancock blending limiter for degree $N = 4$.

The problem consists of a shock impinging on a wedge/ramp which is inclined by 30 degrees. The solution consists of a self similar shock structure with two triple points. The situation is simulated in the rectangular domain $\Omega = [0, 4] \times [0, 1]$, where the wedge/ramp is positioned at $x = 1/6, y = 0$. Defining $\mathbf{u}_b = \mathbf{u}_b(x, y, t)$ with primitive variables given by

$$(\rho, u, v, p) = \begin{cases} (8, 8.25 \cos(\frac{\pi}{6}), -8.25 \sin(\frac{\pi}{6}), 116.5), & \text{if } x < \frac{1}{6} + \frac{y + 20t}{\sqrt{3}}, \\ (1.4, 0, 0, 1), & \text{if } x > \frac{1}{6} + \frac{y + 20t}{\sqrt{3}}, \end{cases}$$

we define the initial condition to be $\mathbf{u}_0 = \mathbf{u}_b(x, y, 0)$. With \mathbf{u}_b , we impose inflow boundary conditions at the left side $\{0\} \times [0, 1]$, outflow boundary conditions both at $[0, 1/6] \times \{0\}$ and $\{4\} \times [0, 1]$, reflecting boundary conditions at $[1/6, 4] \times \{0\}$ and inflow boundary conditions at the upper side $[0, 4] \times \{1\}$. The test is run till $t = 0.2$.

Double Mach Reflection

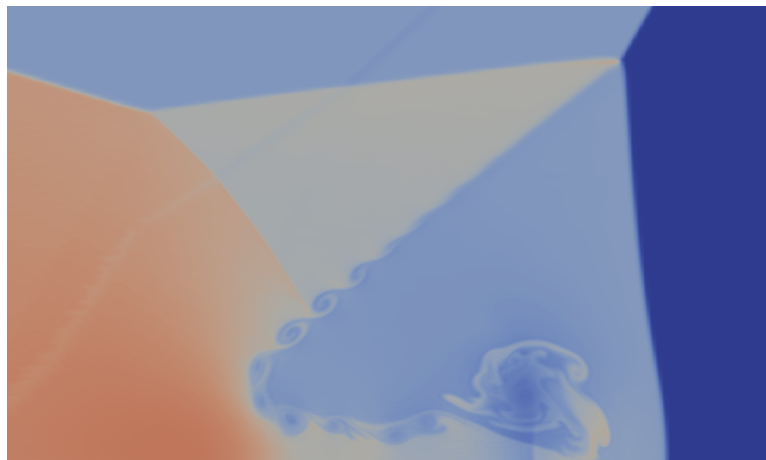


Figure 18. Trixi.jl using First Order blending limiter for Runge-Kutta on a mesh of 568×142 elements with Rusanov flux for $N = 4$.

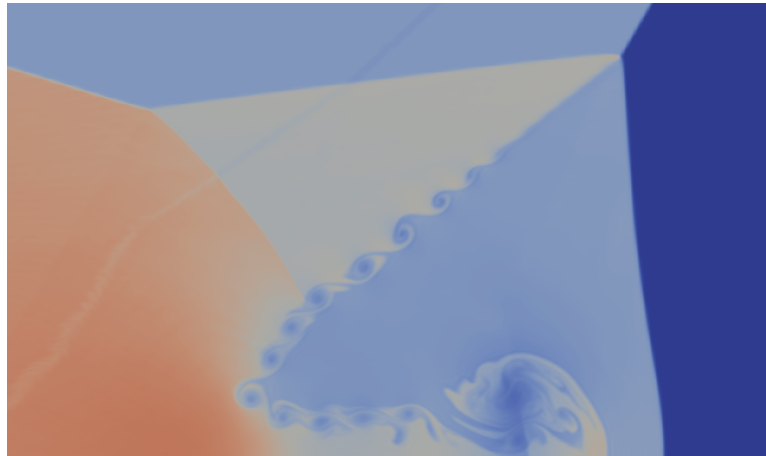


Figure 19. LWFR using MUSCL-Hancock blending limiter with Rusanov flux on a mesh of 568×142 elements for $N = 4$.

Double Mach Reflection

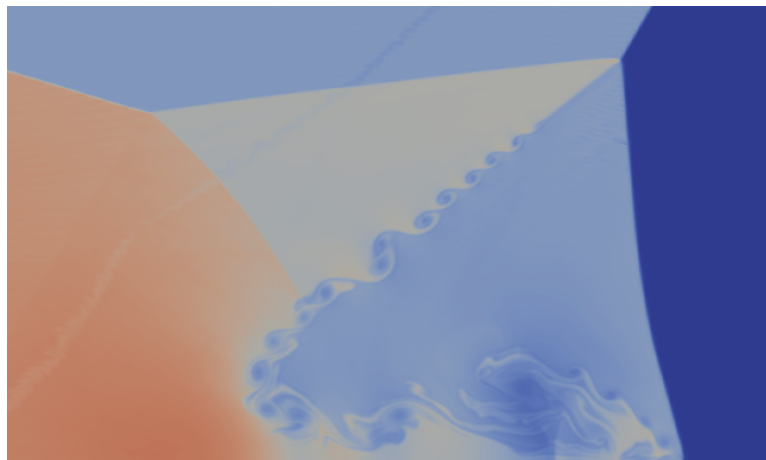


Figure 20. LWFR using MUSCL-Hancock blending limiter with Rusanov flux on a mesh of 568×142 elements for $N = 4$. The smoothness indicator uses $\beta_1 = 0.1$ and $\beta_2 = 1.0$.

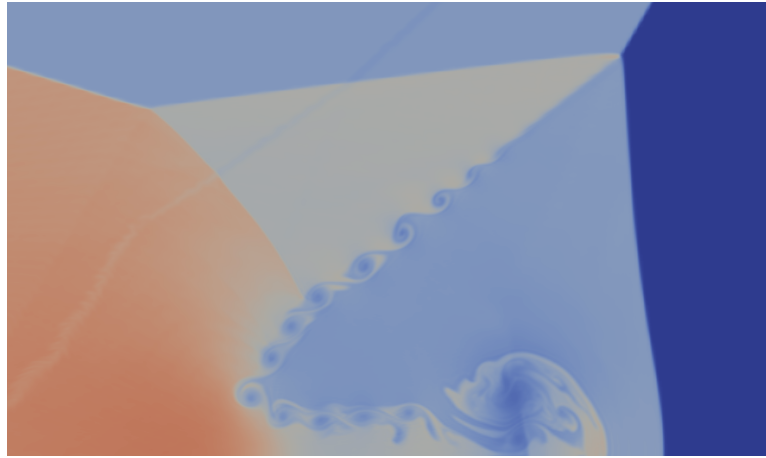


Figure 21. LWFR using MUSCL-Hancock blending limiter with Rusanov flux on a mesh of 568×142 elements for $N = 4$.

Kelvin-Helmholtz Instability

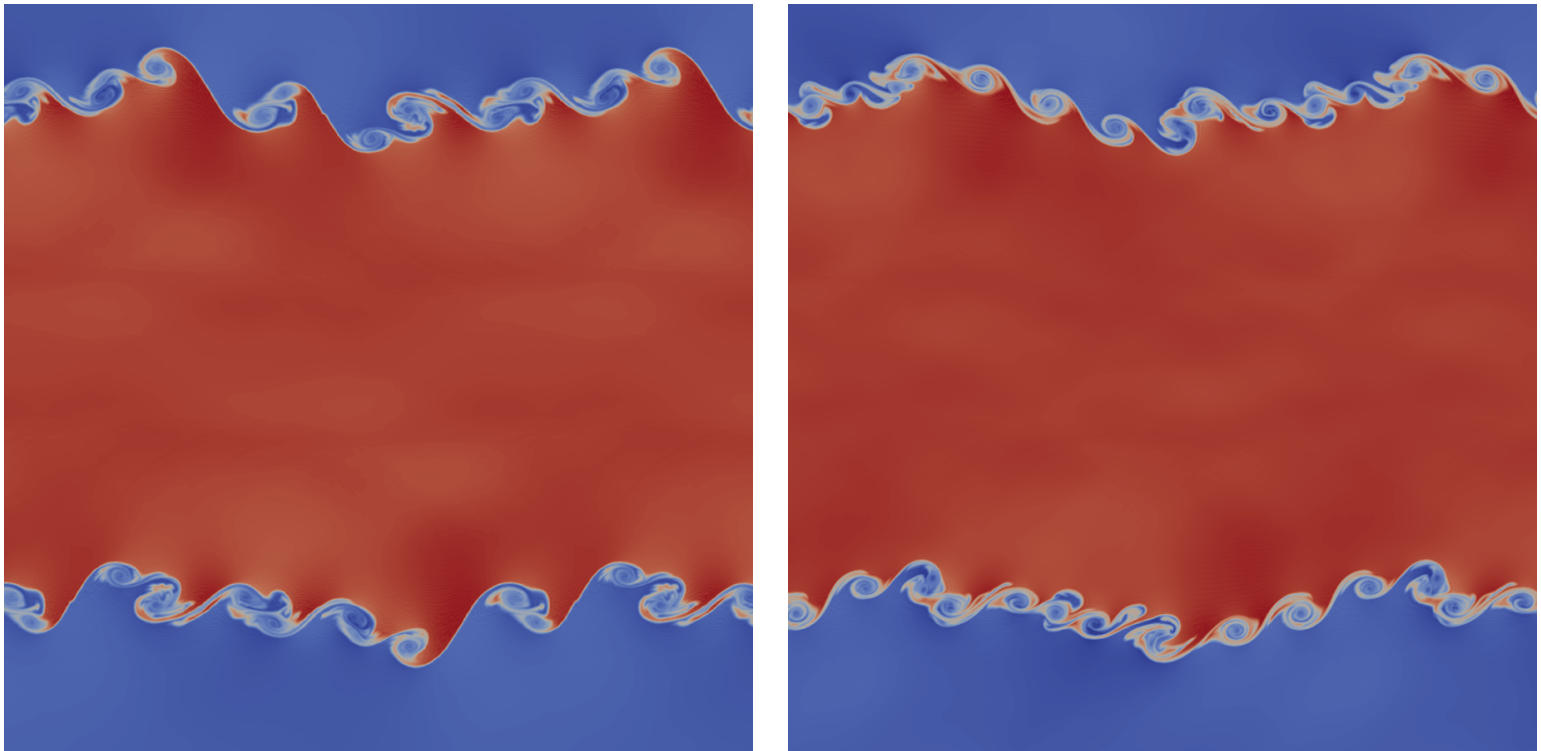


Figure 22. Density profile of Kelvin-Helmholtz test [17, 14] with `Trixi.jl` (left) and `MUSCL-Hancock` (right). Both the tests are with $N = 4$ on a mesh of 256^2 elements.

The test is run on $[0, 1]^2$ with periodic boundary conditions. The initial condition is given by

$$p = 2.5, \quad (\rho, v_1) = \begin{cases} (2, 0.5) & \text{if } 0.25 < y < 0.75, \\ (1, -0.5) & \text{otherwise,} \end{cases}$$
$$v_2(x, y) = w_0 \sin(4\pi x) \left\{ \exp\left[-\frac{(y - 0.25)^2}{2\sigma^2}\right] + \exp\left[-\frac{(y - 0.75)^2}{2\sigma^2}\right] \right\}.$$

where $\omega_0 = 0.1$, $\sigma = 0.05 / \sqrt{2}$, adiabatic index is $\gamma = 7/5$. The solution is plotted at $t = 0.4$.

2-D Sedov blast

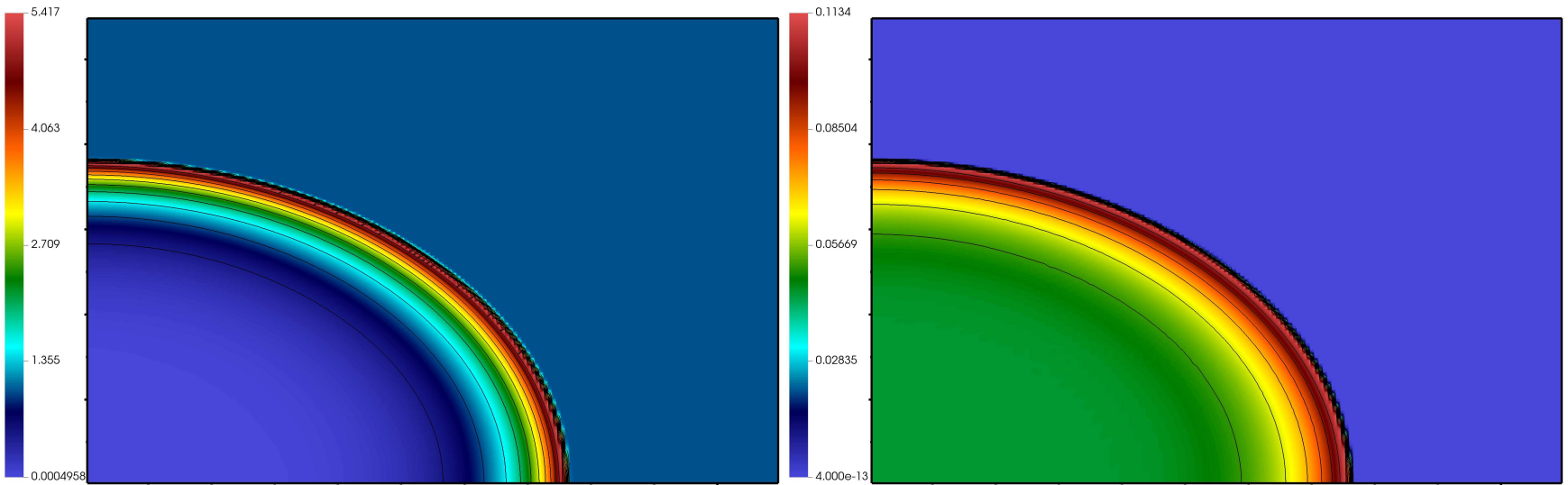


Figure 23. Density and pressure profile of 2-D Sedov blast test case [15] on a mesh of 160^2 elements for degree $N = 4$ to demonstrate admissibility preservation in very severe cases.

We solve on $[0, 1.1] \times [0, 1.1]$ with solid wall boundary conditions on left and bottom, transmissive boundary conditions on right and top. The initial condition is given by

$$\rho = 1.0, \quad v_1 = v_2 = 0.0, \quad E(x, y) = \begin{cases} \frac{0.244816}{\Delta x \Delta y} & x < \Delta x, y < \Delta y, \\ 10^{-12} & \text{otherwise.} \end{cases}$$

The solution is plotted at $t = 0.001$.

Astrophysical jet [4]

We simulate Mach 80 jetflow [4] without radiative cooling, $\gamma=5/3$ on $[0, 2] \times [-0.5, 0.5]$ with initial ambient gas

$$(\rho, u, v, p) = (0.5, 0, 0, 0.4127).$$

The boundary condition on the right, top and bottom are outflow. For the left, we have the high speed jetflow. Mach 80 is simulated by the inflow

$$(\rho, u, v, p) = \begin{cases} (5, 30, 0, 0.4127), & \text{if } y \in [-0.05, 0.05], \\ (0.5, 0, 0, 0.4127), & \text{otherwise,} \end{cases}$$

and Mach 2000 is simulated on the domain $[0, 1] \times [-0.25, 0.25]$ with inflow

$$(\rho, u, v, p) = \begin{cases} (5, 30, 0, 0.4127), & \text{if } y \in [-0.05, 0.05], \\ (0.5, 0, 0, 0.4127), & \text{otherwise.} \end{cases}$$

Astrophysical jet Mach 80 [4]

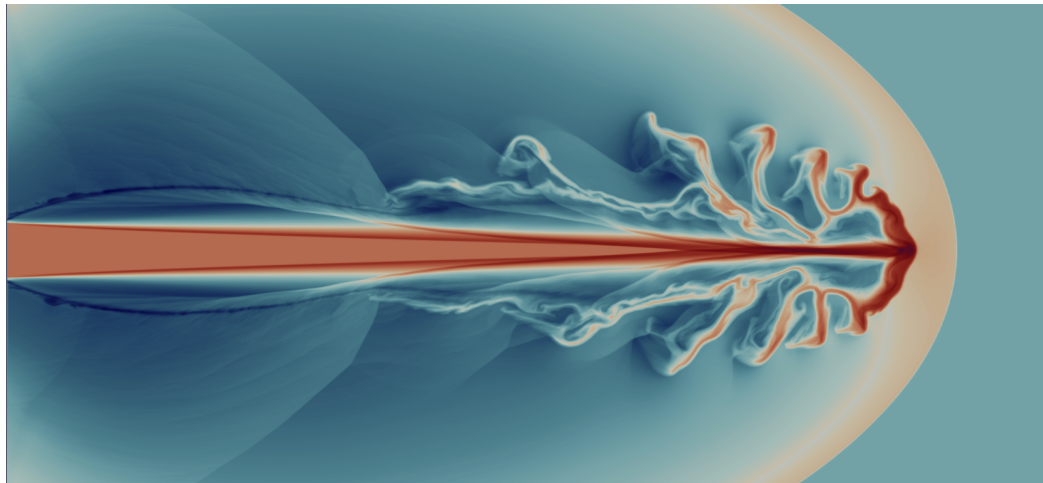


Figure 24. Density profile of Mach 80 jet in log scales on a mesh of 448×224 with $N = 4$

The terminal time is $t = 0.07$.

Astrophysical jet Mach 2000 [4]

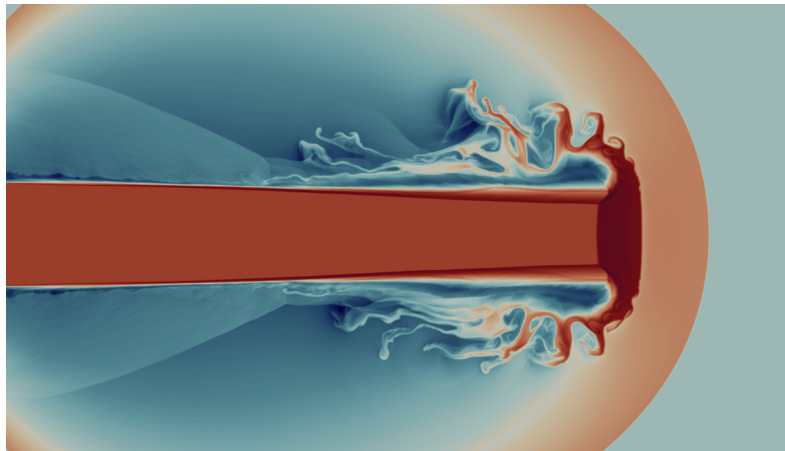


Figure 25. Density profile of Mach 2000 jet in log scales on a mesh of 640×320 mesh with $N = 4$

The terminal time is $t = 0.001$.

Summary and future plans

- A sub-cell based blending limiter based on [5] with MUSCL-Hancock reconstruction has been constructed for Lax-Wendroff schemes.
- The MUSCL-Hancock residual for relevant grids has been proven to be admissibility preserving following the ideas of Berthon [1].
- By correcting Lax-Wendroff time averaged flux during the face loop, an admissibility preserving Lax-Wendroff scheme has been constructed.
- Lax-Wendroff schemes and ADER schemes were proved to be equivalent for linear equations, and mentioned to be *close* for non-linear equations.
- Mild instability for ADER and LW schemes was detected for $N = 4$.

Future Plans

- Extend the scheme to unstructured grids.
- Extend ideas for a MUSCL scheme to RKFR where we would be able to prove entropy stability as in [5].

References

Bibliography

- [1] Christophe Berthon. Why the MUSCL–Hancock scheme is l1-stable. *Numerische Mathematik*, 104(1):27–46, jun 2006.
- [2] Michael Dumbser and Olindo Zanotti. Very high order PNPM schemes on unstructured meshes for the resistive relativistic MHD equations. *Journal of Computational Physics*, 228(18):6991–7006, oct 2009.
- [3] Camille Felton, Mariana Harris, Caleb Logemann, Stefan Nelson, Ian Pelakh, and James A Rossmanith. A positivity-preserving limiting strategy for locally-implicit Lax-Wendroff discontinuous galerkin methods. Jun 2018.
- [4] Youngsoo Ha, Carl Gardner, Anne Gelb, and Chi Wang Shu. Numerical simulation of high mach number astrophysical jets with radiative cooling. *Journal of Scientific Computing*, 24(1):597–612, jul 2005. Funding Information: We would like to thank Jeff Hester for valuable discussions. The authors would like to acknowledge for the following: (1) Research supported in part by the BK21 project at KAIST (Youngsoo Ha); (2) Research supported in part by the Space Telescope Science Institute under grant HST-GO-09863.06-A (Carl L. Gardner); (3) Research supported in part by the National Science Foundation under grant DMS-0107428. (Anne Gelb); (4) Research supported in part by the Army Research Office under grant DAAD19-00-1-0405 and in part by the National Science Foundation under grant DMS-0207451 (Chi-Wang Shu).
- [5] Sebastian Hennemann, Andrés M. Rueda-Ramírez, Florian J. Hindenlang, and Gregor J. Gassner. A provably entropy stable subcell shock capturing approach for high order split form dg for the compressible euler equations. *Journal of Computational Physics*, 426:109935, 2021.
- [6] H. T. Huynh. A Flux Reconstruction Approach to High-Order Schemes Including Discontinuous Galerkin Methods. Miami, FL, jun 2007. AIAA.
- [7] Haran Jackson. On the eigenvalues of the ADER-WENO galerkin predictor. *Journal of Computational Physics*, 333:409–413, mar 2017.
- [8] Guang-Shan Jiang and Chi-Wang Shu. Efficient Implementation of Weighted ENO Schemes. *Journal of Computational Physics*, 126(1):202–228, jun 1996.
- [9] Randall J. LeVeque. High-Resolution Conservative Algorithms for Advection in Incompressible Flow. *SIAM Journal on Numerical Analysis*, 33(2):627–665, apr 1996. Bibtex: LeVeque1996.
- [10] Timur Linde, Philip Roe, Timur Linde, and Philip Roe. Robust euler codes. In *13th Computational Fluid Dynamics Conference*. American Institute of Aeronautics and Astronautics, jun 1997.
- [11] Per-Olof Persson and Jaime Peraire. Sub-Cell Shock Capturing for Discontinuous Galerkin Methods. In *44th AIAA Aerospace Sciences Meeting and Exhibit*, Aerospace Sciences Meetings. American Institute of Aeronautics and Astronautics, jan 2006.
- [12] Jianxian Qiu, Michael Dumbser, and Chi-Wang Shu. The discontinuous Galerkin method with Lax–Wendroff type time discretizations. *Computer Methods in Applied Mechanics and Engineering*, 194(42-44):4528–4543, oct 2005.

- [13] A Rueda-Ramrez and G Gassner. A subcell finite volume positivity-preserving limiter for DGSEM discretizations of the euler equations. In *14th WCCM-ECCOMAS Congress*. CIMNE, 2021.
- [14] Kevin Schaal, Andreas Bauer, Praveen Chandrashekhar, Rüdiger Pakmor, Christian Klingenberg, and Volker Springel. Astrophysical hydrodynamics with a high-order discontinuous Galerkin scheme and adaptive mesh refinement. *Monthly Notices of the Royal Astronomical Society*, 453(4):4278–4300, 09 2015.
- [15] L.I. SEDOV. Chapter iv - one-dimensional unsteady motion of a gas. In L.I. SEDOV, editor, *Similarity and Dimensional Methods in Mechanics*, pages 146–304. Academic Press, 1959.
- [16] Chi-Wang Shu and Stanley Osher. Efficient implementation of essentially non-oscillatory shock-capturing schemes, II. *Journal of Computational Physics*, 83(1):32–78, jul 1989.
- [17] Volker Springel. E pur si muove: Galilean-invariant cosmological hydrodynamical simulations on a moving mesh. *Monthly Notices of the Royal Astronomical Society*, 401(2):791–851, 01 2010.
- [18] Paul Woodward and Phillip Colella. The numerical simulation of two-dimensional fluid flow with strong shocks. *Journal of Computational Physics*, 54(1):115–173, apr 1984.
- [19] Yuan Xu, Qiang Zhang, Chi-wang Shu, and Haijin Wang. The L^2 -norm Stability Analysis of Runge–Kutta Discontinuous Galerkin Methods for Linear Hyperbolic Equations. *SIAM Journal on Numerical Analysis*, 57(4):1574–1601, jan 2019. Bibtex: Xu2019.
- [20] Xiangxiong Zhang and Chi-Wang Shu. On maximum-principle-satisfying high order schemes for scalar conservation laws. *Journal of Computational Physics*, 229(9):3091–3120, may 2010.
- [21] D. Zorío, A. Baeza, and P. Mulet. An Approximate Lax–Wendroff-Type Procedure for High Order Accurate Schemes for Hyperbolic Conservation Laws. *Journal of Scientific Computing*, 71(1):246–273, apr 2017. Bibtex: Zorio2017.

Thank you

Joint Work With

Praveen Chandrashekhar,

TIFR-CAM, Bangalore

Sudarshan Kumar Kenettinkara,

IISER-Trivandrum